Tailoring Microenvironment and Orientation of Immobilized Lactase for Improved Catalysis at Suboptimal pH

Felicia Fianu

Thesis submitted to the faculty of the Virginia Polytechnic Institute and State University in partial fulfillment of the requirements for the degree of

Master of Science in Life Sciences

In

Food Science and Technology

Yifan Cheng (Chair)

Wei Sun

Haibo Huang

December 17, 2024

Blacksburg, Virginia

Keywords: Lactase immobilization, polymers, biotransformation, food waste valorization

Tailoring Microenvironment and Orientation of Immobilized Lactase for Improved Catalysis at Suboptimal pH

Felicia Fianu

ABSTRACT (ACADEMIC)

The U.S. Greek yogurt market has experienced significant growth, rising from 1-2% in 2004 to 40% in 2015, resulting in a large amount of lactose-rich acid whey as a byproduct. Using lactase to transform this waste into valuable products has emerged as a promising solution. Covalent immobilization allows enzymes to be reused and prevents contamination of the product. While immobilizing lactases has been found to enhance their pH and temperature stability, undesired enzyme-substrate interactions can still lead to reduced enzyme activity.

This study investigates novel approaches for enhancing the performance of immobilized lactase enzyme through controlled orientation and microenvironment modification. We utilized initiated chemical vapor deposition (iCVD) to fabricate tailored polymeric thin films as enzyme immobilization supports. A site-specific spycatcher/spytag system was employed for direct immobilization of lactase, while polycationic polymers were incorporated to modify the local chemical environment.

Fourier Transform Infrared (FTIR) spectroscopy confirmed the retention of key functional groups in the polymeric supports. The epoxide-amine ring-opening reaction between the support and enzyme was verified, indicating covalent immobilization. Directed immobilization resulted in significantly improved enzyme activity compared to random

immobilization, particularly at pH 7 and 8. Incorporation of hydrophobic crosslinkers further enhanced the activity of directedly immobilized Lactase, even exceeding that of the free LacZ-ST by 155% at pH 7, while no effect was observed for randomly immobilized LacZ. The inclusion of pH-responsive polycationic moieties in the support enabled LacZ to catalyze at pH 4, where the free enzyme is typically inactive. This study demonstrates the potential of combining controlled enzyme orientation with tailored microenvironments to optimize the performance of immobilized biocatalysts across a broader pH range.

Tailoring Microenvironment and Orientation of Immobilized Lactase for Improved Catalysis at Suboptimal pH

Felicia Fianu

GENERAL AUDIENCE ABSTRACT

With the booming Greek yogurt industry generating substantial amounts of lactose-rich acid whey as a byproduct, there is a pressing need for effective waste management to avoid negative environmental impact. However, the abundance of this acidic byproduct also presents a unique opportunity for product valorization. Lactose, the primary component of acid whey, can be transformed into valuable prebiotics and sweeteners through biotransformation via lactase, an enzyme commonly used for producing lactose-free milk. Nonetheless, the acidic nature of acid whey (~pH 4) inhibits lactase activity, which typically thrives at neutral pH levels (~pH 7).

To tackle this challenge, we explored enzyme immobilization that is, fixing the enzymes on a solid support to improve the stability and reusability of lactase under non-ideal pH environment. Our approach involved using initiated chemical vapor deposition (iCVD) to create specialized polymeric supports for enzyme immobilization via covalent bonds. We employed a site-specific immobilization strategy using the *spycatcher/spytag* system to ensure optimal enzyme orientation, which we hypothesized to be critical for enhancing activity. Additionally, we modified the chemical environment around the immobilized lactase by incorporating a positively charged polymer to allow the local pH to be more neutral than the bulk pH, thus improving the activity of the immobilized lactases.

The results showed that our directed immobilization method significantly improved lactase activity, especially at neutral pH levels, compared to immobilized enzymes with random orientation. Furthermore, by adding positively charged components to the immobilization support, we enabled the immobilized lactase to function even at pH 4, where free lactase is completely inactive. This shows promise for using immobilized lactase to process acid whey without pH adjustment. This research highlights the potential for transforming dairy waste into useful products while addressing the limitations of current enzymatic processes, paving the way for more sustainable practices in food production and biomanufacturing.

Acknowledgement

Primarily, I would like to thank God for His unwavering guidance, strength, and blessings throughout this challenging journey. His grace has been my constant source of inspiration and perseverance.

I extend my deepest gratitude to my advisor, Dr. Yifan Cheng, for his invaluable mentorship, continuous support, and insightful feedback that have been instrumental in shaping this thesis. His expertise and encouragement have been vital to my growth as a researcher.

I am sincerely grateful to my committee members, Dr. Wei Sun and Dr. Haibo Huang, for their constructive advice and novel perspectives that have significantly enhanced the quality of this work.

Special thanks to Geoffrey for his exceptional work in expressing all the proteins crucial for this research. His technical expertise has been indispensable to the success of this project.

I would like to acknowledge my family and friends, especially my brother Dr. Isaac Fianu, whose love and support have been a foundation of strength throughout this journey. Their encouragement has motivated me during challenging times.

I would like to express my appreciation to my lab mates, Babak Faraji, Huida Duan, Hyun Choi, Kobe Tam, and Maye Alyadinov for their camaraderie, intellectual discussions, and support throughout this journey. Their presence made the laboratory a stimulating and enjoyable environment.

My heartfelt thanks go to all the faculty and graduate students in the Food Science and Technology department. Their collective knowledge, encouragement, and friendship have enriched my academic experience immeasurably.

This achievement would not have been possible without the support of all these individuals. I am deeply grateful for their contributions to both my academic and personal development.

Table of Contents

List of figures

List of tables

Attribution

Y.C., W.S., and R.Y. conceptualized the study and formulated the hypotheses. Y.C., with the help of W.S. and R.Y., developed research design and experimental methods. F.F. conducted experiments (synthesized and characterized the iCVD films and analyzed the activity of the immobilized enzymes) and collected all data. H.D. helped with the experiments and verified research reproducibility. J.C. engineered and expressed all the proteins used in the study. F.F. and Y.C. visualized the data and created the figures. F.F. prepared the original draft of the manuscript. Y.C., H.H., and W.S. reviewed and edited the manuscript. Y.C. and W.S. secured financial support for the project.

Introduction

Research indicates that over one-third of all food produced for human consumption is wasted (Giovannucci et al., 2012; Godfray et al., 2010), with losses occurring along the production continuum (Andler & Goddard, 2018). Although the amounts of edible food waste vary geographically, by commodity, and at different points in the supply chain, the amount of food and agricultural waste produced poses a serious environmental burden and continues to be a global challenge. Rapid population growth necessitates the development of creative technological solutions to reduce food waste (Andler & Goddard, 2018).

Disposing of food processing waste streams directedly into water bodies and wastewater treatment facilities is illegal due to their high biological oxygen demand (USA EPA, 1999). Greek yogurt acid whey exhibits a notably high biological oxygen demand, ranging from 52,400 to 62,400 mg/L, posing significant challenges in terms of environmentally friendly disposal (Menchik et al., 2019). Nonetheless, food processing waste streams are rich in components such as lipids, carbohydrates, and proteins that have the potential to be modified into value-added goods, thus turning waste streams into potential revenue streams. The oxidation, hydrolysis, acylation, and phosphorylation of carbohydrates, the deamination and glycosylation of proteins, the hydrogenation and esterification of lipids, and the deamination and glycosylation of carbohydrates are a few examples of significant changes (Alissandratos & Halling, 2012; Fang et al., 2002; Walle, 2009) applied to some components of food waste streams.

There has been a notable uptick in the production of acid whey, primarily driven by the rising demand for Greek yogurt and acid-coagulated cheeses (Andler & Goddard, 2018;

Rocha-Mendoza et al., 2021). Whey is an aqueous component of milk, also referred to as the liquid that remains once fat and casein have been separated. It primarily comprises soluble constituents, such as lactose, soluble salts, globular proteins, and other elements (Chandrapala et al., 2016; P. M. R. Guimarães et al., 2010). The production of acid whey has undergone a surge in recent years, propelled by the increasing production of Greek yogurt from 1-2% in 2004 to 40% in 2015 (Andler & Goddard, 2018; Rocha-Mendoza et al., 2021). Since 2009, there has been heightened demand for Greek yogurt in the United States, driven by health-conscious consumers seeking high-protein, low-fat, and convenient dietary options (Becker et al., 2017). Presently, Greek yogurt commands a majority share of the yogurt market in the United States and holds the distinction of being the most favored yogurt style purchased in 2019 (Mintel, 2019). In the process of making Greek yogurt, 100 units of milk yielded 33 units of yogurt and 67 units of acid whey (Erickson, 2017). To put this into perspective, in 2015, a staggering 771,000 tons of Greek yogurt were produced, generating nearly 1.5 million tons of acid whey in parallel (Erickson, 2017). Acid whey, the major by-product of the dairy industry, has historically posed sustainability challenges due to the high volumes produced and the constituents which have adverse implications on the environment when disposed directedly into water bodies or wastewater treatment plants (Rocha-Mendoza et al., 2021). Greek yogurt acid whey exhibits a notably high biological oxygen demand, ranging from 52,400 to 62,400 mg/L, posing significant challenges in terms of environmentally friendly disposal (Menchik et al., 2019). Moreover, due to its elevated lactic acid content and low pH, spray-drying acid whey proves to be a complex task, as a huge portion of the lactose tends to crystallize (Bylund, 2015).

This sheds light on the need to explore ways individual components such as lactose, which is a major constituent in acid whey, can be valorized. In addition, the increased production of Greek yogurt and cottage cheese exerts increasing pressure on the dairy sector to pioneer inventive and sustainable approaches for repurposing acid whey (Zotta et al., 2020).

Within the industry, efforts have been made to harness acid whey on-site through the utilization of ultrafiltration techniques and biodigesters. This approach helps to reduce transportation expenses as well as providing an energy source for the facility (Rocha-Mendoza et al., 2021). On-site acid whey processing using ultrafiltration and biodigesters faces high costs, energy demands, process complexity, scalability issues, membrane fouling, environmental concerns, and underutilization of byproducts (Rocha-Mendoza et al., 2021). In recent times, dairy companies dedicated to environmental sustainability have been actively seeking ways to manage acid whey more responsibly. Their efforts encompass a range of strategies, such as extracting valuable components from acid whey and implementing cost-effective filtration methods (Smithers, 2015).

Table 1: Trends in Acid whey and its component applications

Utilization	Process	Purpose	Challenges	References
Use as fertilizer	Direct application or mixing up with manure before application on farmlands	To increase the mineral content of the farmland	Low pH of acid whey tends to be more hazardous to plants. Modification of the pH is required.	(Ketterings, 2017)
Use in animal feed	Mixing with silage	To serve as a wetting agent and enrich the feed with nutrients	Low pH and mineral composition of acid whey tend increase the salt toxicity of animals as well as degrading of animal stalls.	(Shurson, 2009)
Used in fermented milk beverages	Mixing with milk	Used as a major component in producing fermented milk drinks like yoghurt. due to its composition	The flavor, sourness and saltiness of acid whey tends to reduce consumer acceptability of products having acid as the main component	(Lievore et al., 2015)
Biofuel production	Fermentation of lactose in acid whey using microorganisms (*Kluyveromyces lactis*, *Kluyveromyces marxianus*, and *Candida pseudotropicalis)*.	It is used to produce ethanol, methane (biogas), amino acids, and organic acids, among others.	To enhance the outcome, it is necessary to process the acid whey through methods such as ultrafiltration, reverse osmosis, or a combination of both, to concentrate the lactose.	(Das et al., 2016; P. M. R. Guimarães et al., 2010)

These inherent complications associated with the disposal of acid whey add a layer of complexity to its valorization. Consequently, further research is imperative to explore potential applications for this abundant by-product. Traditional methods for these alterations demand a chemical catalyst, substantial energy input, low reaction selectivity, and produce byproducts, especially when applied to complex matrices like food waste streams (Rocha-Mendoza et al., 2021).

Biocatalysis employing the use of enzymes or microorganisms is rising as a promising strategy to overcoming the limitations of the traditional approaches for waste valorization (Andler & Goddard, 2018). Enzymes play a crucial role in lowering the activation energy of biochemical reactions, thereby accelerating the rate of these reactions (Immobilization of Enzymes and Cells SECOND EDITION, n.d.). There are widespread applications of

enzymes across various industries, including food, chemicals, pharmaceuticals, medicine, textiles, and agriculture. However, a key drawback of enzymes is their susceptibility to instability, particularly when exposed to extreme temperature and pH environments. This challenges the beneficial attributes of enzymes and their extensive use in various industrial applications, thus frequently hindering their long-term operational durability, shelf life, recovery and reuse (J. C. S. D. Santos et al., 2015; Sirisha et al., 2016). Immobilization of enzymes has given light as an effective approach to address the issues associated with the use of enzymes for biotransformation. In reality, the primary obstacle in industrial biocatalysis is the creation of biocatalysts that are both stable and robust, and preferably not soluble in the reaction medium (Datta et al., 2013).

Immobilizing enzymes involves binding enzymes to a supporting material, restricting their free movement in a solution (CHIBATA, 1979). This technology offers a promising solution to enhance enzyme stability and reusability. Notably, the most significant advantage of enzyme immobilization is the improvement in thermal and pH stability, enabling enzymes to be used multiple times and facilitating their separation from reaction mixtures (Homaei et al., 2013; D. M. Liu et al., 2018). Over the past four decades, there has been considerable progress in the development of enzyme immobilization technology. However, the broader adoption of immobilized enzymes in industrial processes necessitates the exploration of new methods and a deeper understanding of existing techniques (Zahirinejad et al., 2021) to optimize paramount parameters to achieve sustainable and efficient biocatalysis. Furthermore, the utilization of immobilization methods has the potential to enhance various enzyme characteristics, including their activity, stability, and specificity (Barbosa et al., 2015; J. C. S. dos Santos

et al., 2015). As a result, enzyme immobilization has emerged as a crucial strategy for creating economically feasible industrial biocatalysts with optimal performance (Sheldon, 2011).The careful choice of an appropriate immobilization procedure is of utmost importance to fully capitalize on these benefits (J. C. S. D. Santos et al., 2015; Sheldon & van Pelt, 2013). For example, Paiva et al. observed an increase in the Michaelis Menten K_m values of immobilized β-galactosidase (lactase) into alginate matrix as compared to the soluble lactase (Paiva et al., 2023). K_m is the substrate concentration at which we obtained half the maximum reaction rate of the enzyme kinetics. A lower K_m is desirable as it provides an estimate that there is a higher binding affinity between the enzyme active site and the substrate. The observed rise in K_m values can be accounted for by a decrease in the enzyme's affinity for the substrate which was attributed to factors associated with the enzyme's confinement process and the challenges encountered by the substrate in accessing the enzyme's active sites (Klein et al., 2018a). In a study by Kumar et al., they reported a two-fold increase in K_m values for immobilized urease in alginate and chitosan matrices, while the maximum rate (V_{max}) values remained relatively unchanged (Kumar et al., 2009a). The authors primarily attributed this alteration in K_m values to the hindrance of substrate diffusion caused by the presence of the alginate matrix. The matrix often hinders the free movement of the substrate, thereby prolonging the time it takes for the substrate to reach the catalytic site (Paiva et al., 2023).

Covalent immobilization is effective at creating strong enzyme-surface bonds, but it is prone to undesired interactions that reduce enzyme activity (Barbosa et al., 2014; Kim et al., 2006; Mateo et al., 2007). Traditional immobilization methods lack control over enzyme orientation, limiting the ability to minimize unwanted interactions, optimize

stability, and enhance active-site accessibility (Hernandez & Fernandez-Lafuente, 2011; Mateo et al., 2007). Developing technologies for site-specific enzyme immobilization will offer numerous benefits, as specific attachment sites can reduce undesired interactions and improve stability. Precise control of immobilization orientation can also mitigate active-site hindrance and provide insights into enzyme-surface interactions (Friedel et al., 2007; Talasaz et al., 2006; Wei & Knotts, 2011; Zhuang et al., 2009). Past covalent site-specific immobilization techniques have had limitations on available attachment sites, and alternative methods rely on noncovalent approaches (Kalia et al., 2007; Lim et al., 2014; Seo et al., 2011).

Polymers stand out as exceptionally promising candidates for various applications due to their notable attributes such as a high strength-to-weight ratio, stiffness, toughness, ductility, and cost-effectiveness (Celentano et al., 2020; La Mantia et al., 2021; G. Y. Liu et al., 2021; Marć et al., 2021). Furthermore, they possess a broad range of operating temperatures, provide high thermal/electrical insulation, and demonstrate resilience against corrosion and light. Additionally, their relatively straightforward derivatization allows for precise adjustments to their properties (Cruz Sanchez et al., 2017; Khoo et al., 2020; M. Subramaniam, 2019; Ng et al., 2020). Polymeric thin films offer significant advantages over bulk polymers. Compared to producing bulk polymers, making polymeric thin films is quicker and requires fewer chemicals (Gürsoy, 2021). They allow tailoring surface properties for specific functionalities without compromising the overall mechanical integrity or structural stability of the material (Ansari & Husain, 2012; Zahirinejad et al., 2021). This flexibility in design contributes to the versatility and effectiveness of polymer thin film coatings in diverse industrial and research contexts.

The initiated chemical vapor deposition (iCVD) method was developed as a dry method for creating polymeric thin films. iCVD thin films have unique properties, such as functionality, uniformity, conformity, and being free of pinholes (de Bruin, 2018; Nemani et al., 2018). iCVD, organic thin films, can be synthesized on various substrate types at high deposition rates due to their distinctive deposition mechanisms. This mechanism involves a classically free radical polymerization reaction, which is typically conducted in a container with a mixture of monomers, initiators, and a suitable solvent to produce bulk polymers. In iCVD, this reaction occurs on a cooled substrate surface in a dry vacuum environment (Asatekin et al., 2010; Gleason, 2015; Yılmaz et al., 2021). iCVD is a subtype of the well-known hot filament activated chemical vapor deposition (CVD) method, which uses heated filaments to provide the energy needed to initiate the chemical reactants (initiator) to form free radicals. These free radicals react with adsorbed monomers on a cooled substrate to form the robust polymeric film (Yılmaz et al., 2021) with specific surface chemistries. Primary radicals generated from the thermal activation of initiators (typically *tert*-butyl peroxide) diffuse through the iCVD reacting chamber to the cooled substrate surface, where they are adsorbed along with the monomer molecules. The adsorption process in iCVD is physical and does not wet the substrate surface. The adsorbed molecules react to creating dense polymers in the form of thin films. iCVD offers a broader array of functional groups and enables finer control over polymer chemistry (Yılmaz et al., 2021). iCVD has successfully deposited chemically sensitive functional groups, like the glycidyl group (Decher & Schlenoff, 2012b) and the pentafluoro phenyl group(N. Marı´-Buye´, 2009), at high surface densities due to its low process temperature. Generally, iCVD polymers typically retain 100% of the functional groups present in the

monomers, except for the vinyl groups (Coclite et al., 2013) which function as the polymerization sites. The high retention of monomer pendent group in iCVD polymer films makes iCVD films the best polymeric nanolayer support for achieving high enzyme immobilization density and high pH buffering capacity. Over time, a wide range of functional polymers have been applied to various substrates for different purposes, including antimicrobial, stimuli-responsive, superhydrophobic, and zwitterionic applications (Khlyustova et al., 2020a; Yang & Gleason, 2012). Furthermore, the iCVD process is not limited to specific materials or geometries and can cover 3D features and micro- and nano-scale surfaces (Alrifaiy et al., 2012; Teles & Fonseca, 2008). iCVD provides a robust technique in creating uniform and high-quality films on a variety of surfaces (Chen et al., 2016; Gleason, 2015), including flexible substrates like 96-well plates and 2D materials for biological applications such as enzyme immobilization.

The central hypothesis for this research is that covalent immobilization of bioengineered lactase with a specific orientation onto thin polymeric nanolayer support with precise surface chemistry and physics will significantly increase the stability, reusability and recovery of the immobilized lactase in low pH conditions. The specific objectives for this project are outlined below.

1. Investigate the impact of specific orientation imposed by the Spycatcher/Spytag coupling on the performance of immobilized lactase.
2. Investigate how the physicochemical properties of polymeric nanolayers affect the performance of immobilized lactase.

   2a. Examine the impact of different cross-linkers incorporated in iCVD coatings on the stability and efficacy of immobilized lactases.

2b. Explore the impact of buffering capacity and ionization of surface moieties on polymeric nanolayers fabricated using iCVD with the inclusion of pH-responsive monomer on immobilized lactase activity.

3. Assess the impact of employing solution-phase polymerization of Self-Assembly Monolayers (SAMs) as opposed to vapor phase polymerization (iCVD) on the performance of immobilized lactase by examining changes in physicochemical characteristics, including buffering capacity and ionization of the surface functional groups generated within the monolayers.

Manuscript 1

Tailoring Microenvironment and Orientation of Immobilized Lactase for Improved Catalysis at Suboptimal pH

Felicia Fianu[1], Junxing Chen[2], Huida Duan[1], Huang Haibo[1], Rong Yang[3], Wei Sun[2], Yifan Cheng[1,3]*

1. *Virginia Polytechnic Institute and State University, Department of Food Science and Technology, Blacksburg, VA 24061*
2. *Virginia Polytechnic Institute and State University, Department of Biochemistry, Blacksburg, VA 24061*
3. *Cornell University, Smith School of Chemical and Biomolecular Engineering, Ithaca, NY 14853*

Abstract

The U.S. Greek yogurt market has experienced significant growth, rising from 1-2% in 2004 to 40% in 2015, resulting in a large amount of lactose-rich acid whey as a byproduct. Using lactase to transform this waste into valuable products has emerged as a promising solution. Covalent immobilization allows enzymes to be reused and prevents contamination of the product. While immobilizing lactases has been found to enhance their pH and temperature stability, undesired enzyme-substrate interactions can still lead to reduced enzyme activity.

This study investigates novel approaches for enhancing the performance of immobilized lactase enzyme through controlled orientation and microenvironment modification. We utilized initiated chemical vapor deposition (iCVD) to fabricate tailored polymeric thin films as enzyme immobilization supports. A site-specific spycatcher/spytag system was

employed for directed immobilization of lactase, while polycationic polymers were incorporated to modify the local chemical environment.

Fourier Transform Infrared (FTIR) spectroscopy confirmed the retention of key functional groups in the polymeric supports. The epoxide-amine ring-opening reaction between the support and enzyme was verified, indicating covalent immobilization. Directed immobilization resulted in significantly improved enzyme activity compared to random immobilization, particularly at pH 7 and 8. Incorporation of hydrophobic crosslinkers further enhanced the activity of directedly immobilized LacZ, even exceeding that of the free LacZ by 155% at pH 7, while no effect was observed for randomly immobilized LacZ. The inclusion of pH-responsive polycationic moieties in the support enabled LacZ to catalyze at pH 4, where the free enzyme is typically inactive. This study demonstrates the potential of combining controlled enzyme orientation with tailored microenvironments to optimize the performance of immobilized biocatalysts across a broader pH range.

1.0 Introduction

The briskly growing U.S. Greek yogurt market, (1-2% percent from 2004 to 40% in 2015) has created massive volumes of lactose-rich acid whey as a byproduct. The ratio of Greek yogurt produced to acid whey byproduct is 1:2 or 1:3(Andler & Goddard, 2018; Goddard & Hotchkiss, 2007). Lactose is the main constituent (3.5% wt/wt) of the acid whey generated from the US Greek yogurt production. Biotransformation of lactose by lactase has emerged as a promising strategy for valorizing lactose rich waste streams into prebiotics and non-nutritive sweeteners (Andler & Goddard, 2018; Goddard & Hotchkiss, 2007). However, the high acidic content of acid whey (pH ~ 4) does not create an optimum environment for lactase (pH ~ 7) activity (Goddard & Hotchkiss, 2007) thus reducing the recovery and reusability of lactase for extended period. This ineffectiveness of lactase in harsh environments hinders the utilization of biocatalysis to its full potential. Immobilization has developed to be an auspicious approach to increase the operational functionality of biological molecules in extended pH and temperature stipulations (Datta et al., 2013; Homaei et al., 2013). In contrast to enzymes in their soluble state, immobilized enzymes exhibit greater stability and offer the advantage of easy separation from both the reaction mixture and the end product. However, this leads to a notable reduction in enzyme usage (F. F. Freitas et al., 2012). Lactase immobilization has been accomplished using a range of diverse techniques, such as physical adsorption, encapsulation, gel entrapment, crosslinking, and covalent attachment (Kierstan & Coughlan, 1991; Sheldon, 2011; Sheldon & van Pelt, 2013; Wang et al., 2021). Previous studies have shown that covalent immobilization provides the most effective method for creating robust and durable connections between enzymes and surfaces. Nevertheless,

it is also most susceptible to unintended interactions between the surface and the enzyme, which can lead to a loss of immobilized enzyme activity (Barbosa et al., 2015; Kim et al., 2006; Mateo et al., 2007). Covalent immobilization of enzymes using polymeric supports is liable to undesirable enzyme-surface reactions mostly attributable to the polymeric support (Goddard & Hotchkiss, 2007; Homaei et al., 2013; Wu et al., 2015). To make immobilized enzymes more economically competitive for practical use, it is essential to minimize the expenses associated with the immobilization process (F. F. Freitas et al., 2012) as well as utilizing promising efficient immobilization techniques. Traditionally, immobilization techniques have common limitations in their inability to precisely control how enzymes attach to the surface. This limitation hinders efforts to reduce unwanted interactions between enzymes and surfaces, optimize enzyme stability, and ensure easy access to the enzyme's active site (Hernandez and Fernandez-Lafuente, 2011; Mateo et al., 2007b). It can however be inferred that the catalytic efficiency of immobilized enzymes is mostly affected by the enzyme orientation and the local microenvironment generated by the nanolayer support.

The development of technologies that allow for site-specific enzyme immobilization at specific points in the protein have opened numerous possibilities. Previous modeling studies have suggested that selecting particular attachment sites can minimize undesirable enzyme-surface interactions and enhance the thermodynamic stability of immobilized proteins and enzymes (Friedel et al., 2007; Talasaz et al., 2006; Wei & Knotts, 2011; Zhuang et al., 2009). Furthermore, precise control of immobilization orientation can mitigate the hindrance of the enzyme's active site after immobilization and provide a deeper understanding of how enzymes interact with their support surfaces.

To address this challenge of immobilization, various site-directed immobilization techniques have been developed, such as biorthogonal chemical methods like oxime ligation, cycloaddition, chemoenzymatic coupling, and the use of fusion proteins with self-ligating protein tags (Walden et al., 2019). Although these site-directed immobilization strategies significantly improve the activity of immobilized enzymes, they often require the use of costly unnatural amino acids (Gao et al., 2023). One widely used site-specific protein-reactive pair is spycatcher/spytag, derived from *Streptococcus pyogenes*. This system forms a spontaneous isopeptide bond between Lys31 and Asp117 and has been extensively applied in protein labeling, purification, antibody capture, and the oriented immobilization of antibodies (C. Li et al., 2021; L. Li et al., 2014; Zakeri et al., n.d.).

iCVD is a dry method for creating uniform, pinhole-free polymeric thin films on various substrates. It uses a free radical polymerization process in a vacuum, where heated filaments activate initiators to generate radicals that react with adsorbed monomers on a cooled substrate. The use of iCVD to form thin films on solid substrates provides a robust technique to control polymer film physics and chemistry. Unlike traditional liquid phase polymerization, iCVD offers precise and conformally thin polymer film coatings, operates at lower temperatures to protect a variety of substrates, minimizes chemical waste, and yields high-purity films with customizable functional properties (Gleason, 2015; Martin et al., 2007; Yılmaz et al., 2021).

SAMs, which refer to arranged molecular assemblies that are created through the adsorption of an active surfactant onto a solid surface (Ulman, 1996) represent a distinctive category of surfaces with the capability to showcase various unique surface chemistries, providing an innovative approach for investigating interactions between cells

and biomaterials (Jones et al., 2008). The biomimetic and biocompatible properties of SAMs hold potential for applications in chemical and biochemical sensing, offering prospects in these areas(Schreiber, 2004; Ulman, 1996). Functionalized silane monolayers, particularly those incorporating epoxy-silanes and alkyl amines, have become highly prominent due to their efficacy in securely anchoring biomolecules like proteins, enzymes, and DNA (Goddard & Hotchkiss, 2007).

In this study,

i. We utilized the robust iCVD technique to fabricate homopolymer and copolymer polymeric thin films with tailored surface functionalities as well as solution-phase synthesis of SAMs with different end groups for both random and directed immobilization of lactase.
ii. We utilized the site-specific enzyme orientation method through the application of spycatcher/spytag system for directed immobilization of lactase.
iii. In addition, we modified the chemical microenvironment of immobilized lactase by incorporating a polycationic polymer within the polymeric support network.

2.0 Chemical reagents

All precursors, including iCVD monomers (GMA, EGDMA, DVB, DMAEMA), iCVD initiator (TBPO) were purchased from Sigma-Aldrich Inc. (St. Louis, MO, USA) and SAMs (GPTMS, DMAPTMS) from Fisher Scientific Company LLC (3970 Johns Creek Ct Ste 500 Suwanee, Georgia 30024-1297, USA) and used without further purification. Specifically, the purity of the iCVD monomers are GMA (97.0%, hydroquinone monomethyl ether ~ 0.01 % as stabilizer), EGDMA (98%, 90-110 ppm monomethyl ether hydroquinone as anti-polymerization agent), DVB (80%), DMAEMA (98%, 700-1000 ppm monomethyl ether hydroquinone as inhibitor); iCVD initiator TBPO (98%), SAMs monomers, GPTMS (98%, TCI America) and DMAPTMS (96%, TCI America).

2.1 Fabrication of immobilization support using iCVD

This study employed thin polymeric nanolayer films, synthesized by initiated chemical vapor deposition (iCVD), as the immobilization supports for lactase. Monomers such as glycidyl methacrylate (GMA) were used to provide binding sites for lactase immobilization. Ethylene glycol Dimethacrylate (EGDMA) and divinylbenzene (DVB) were utilized as crosslinkers to stabilize the immobilization support, 2-(N, N-Dimethylamino) ethyl methacrylate (DMAEMA), a polycationic polymer, was incorporated to offer buffering capacity in response to changes in pH of the reaction media. Tert-butyl peroxide served as the initiator, consistent with typical iCVD polymerization processes(Gleason, 2019; Im et al., 2009). The precursors for the immobilization support with specific surface chemistries were vaporized and introduced into the iCVD chamber at a total flow rate ranging from 3 to 5 sccm. The flow rate of TBPO, the stage temperature and the total process pressure were maintained at 0.6 sccm, 35 °C and 0.6 Torr, respectively, for all

depositions. The gas flow rates and the kinetic parameters for the iCVD depositions are summarized in Table S1 and Table S2, respectively. The polymerization reaction was initiated by resistively heating a filament array to a temperature of 220 °C to cause the formation of primary free radicals from TBPO. Polystyrene 96-well plates (Corning(Tm) 96 Well Eia/Ria Assay Microp) were used as substrates for lactase immobilization and enzyme kinetic experiments. The 96-well plates were placed on a custom-made aluminum plate, which fits well with the bottom of the 96-well plates, to facilitate heat transfer to the reactor cooling stage during the coating process. During each deposition, a silicon substrate placed atop the 96-well plate was used for *in situ* film thickness monitoring via an interferometer equipped with a He-Ne laser and wavelength range of 350 – 700 nm (Thorlabs Inc., Newton, NJ, USA).

2.2 Fabrication of Self-Assembly Monolayers (SAMs)

Two distinct silane compounds, 3-Glycidyloxypropyltrimethoxysilane (GPTMS) and 3-[(N, N-Dimethylamino)-propyl]trimethoxysilane (DMAPTMS), were employed to mimic critical functional groups in iCVD polymers. To enhance coupling with Self-Assembled Monolayers (SAMs), surface modification of both 96-well plates and silicon wafers were pretreated with oxygen plasma for 3 minutes at power of 45 W and 500 - 900 mTorr chamber pressure (Harrick Plasma Inc, NY, USA). This approach introduced hydroxyl functional groups onto the microplate surface, enabling covalent -O-Si-O- bonding of SAMs with Hydroxyl groups via silanization reactions.

GPTMS and DMAPTMS working solutions (1 %v/v in ethanol) were prepared separately by stirring at 350 rpm at 20 ^{o}C and atmospheric pressure for 1 hour. The working solutions were combined in a way that to produce a GPTMS-DMAPTMS mixed solution with the

molar composition of GPTMS (74%) and DMAPTMS (26%), mirroring the composition of DMAEMA in iCVD-fabricated film, pGD(25). Plasma treated substrates (96-well plate and silicon wafer) were coated with either the GPTMS working solution or the GPTMS-DMAPTMS mixed solution by submerging the substrates for 18 hours at room temperature. The SAMs-functionalized substates were rinsed with ethanol followed by distilled water, and then dried as described previously (Faucheux et al., 2004).

2.3 Ellipsometry of iCVD films

The thickness of the deposited iCVD films on silicon wafers was measured *ex-situ* using the J.A. Woollam alpha-SE Spectroscopic Ellipsometer (Lincoln, NE, USA) at three distinct incident angles (65°, 70°, and 75°). The film thickness was regressed using the Cauchy-Urbach model. This step was undertaken to validate the film thickness before proceeding with lactase immobilization and subsequent characterizations. Thickness measurement was done at multiple spots on a sample and averaged.

2.4 FTIR Characterization

FTIR analysis was conducted to verify the presence and preservation of characteristic functional groups in the iCVD-synthesized polymer films. The FTIR spectroscopy of all immobilization supports was performed utilizing a Thermo Scientific Nicolet iS50 Model (Austin, TX, USA). For compositional characterization of copolymers, FTIR analysis was conducted in transmission mode. Attenuated Total Reflectance Fourier Transform Infrared Spectroscopy (ATR-FTIR) was performed using the Thermo Scientific Nicolet iS50 Model equipped with a VariGATR grazing angle ATR accessory (GAT-V-N18, Harrick Scientific Products, NY). The incident angle of the ATR accessory, 60° was used. A MCT detector cooled with liquid nitrogen was utilized over the spectral range of 600-

4000 cm^{-1} with a resolution of 4 cm^{-1} with measurements averaged over 128 scans to improve the signal-to-noise ratio. Baseline correction was applied by subtracting a background spectrum obtained from an uncoated Si wafer substrate.

2.5 Bioengineering of enzymes

2.5.1 Cloning of pBAD-LacZ plasmid, pBAD -LacZ-spy-tag plasmid and pBAD-spycatcher plasmid

To generate the pBAD -LacZ-WT plasmid, the Beta-galactosidase (LacZ) (Uniprot ID: P00722) encoding gene was synthesized by amplifying the colony PCR with the Primer pair of LacZ-WT-Nde I-F and LacZ-LacZ-WT-6xHis-R, digested with NdeI and HindIII, and ligated into pBAD vector pretreated with the same restriction.

To generate the pBAD-LacZ-spytag plasmid, the template for spy-tag and GS linker were PCR-amplified using primer spy-tag-GSlinker-F and spy-tag-GSlinker-R to yield double stranded DNA and then recombinant with the lacZ-WT template that PCR amplified by primer pBAD-LacZ-WT-spy-F and pBAD-LacZ-WT-spy-R on N-terminal.

To generate the pBAD-spycatcher plasmid, the spycatcher sequence (GenBank: AFD50637.1) was codon optimized and synthesized by IDT, the template was amplified with the Primer pair of spycatcher-Nde I-F and spycatcher-Hind III-6xHis-R, digested with NdeI and HindIII, and ligated into pBAD vector pretreated with the same restriction.

2.5.2 Protein Expression and Purification

LacZ

pBAD-LacZ plasmid and pBAD-LacZ-spy-tag plasmids were transformed into DH10B E. coli chemical competent cells. The transformants were plated on an LB-Amp100 agar

plate and incubated overnight at 37 °C. A single colony was inoculated into 5 mL of LB-Amp100 and cultured overnight at 37 °C. On the following day, 1 mL of overnight cell culture was diluted into 5 L LB- Amp100 and agitated vigorously at 37 °C. When OD600 reached 0.4~0.6, the cell culture was induced with 0.2% arabinose, then incubated at 37 °C for 24 hours. Cell pellets were collected by centrifugation at 7000 g for 15 min at 4 °C and stored at −80 °C.

Spycatcher

pBAD-spycatcher plasmid was transformed into DH10B E. coli chemical competent cells. The transformants were plated on an LB-Amp100 agar plate and incubated overnight at 37 °C. A single colony was inoculated into 5 mL of LB- Amp100 and cultured overnight at 37 °C. On the following day, 1 mL of overnight cell culture was diluted into 5 L LB- Amp100 and agitated vigorously at 37 °C. When OD600 reached 0.4~0.6, the cell culture was induced with 0.2% arabinose, then incubated at 18 °C for 24 hours. Cell pellets were collected by centrifugation at 7000 g for 15 min at 4 °C and stored at −80 °C.

His-tag Protein Purification

Above cell pellets were resuspended in 14 mL lysis buffer (20 mM Tris-HCl pH 8.8, 400 mM NaCl, 20 mM imidazole, and proteinase inhibitors). The cell suspension was lysed at 4 °C for 30 min. Cell lysate was sonicated with Branson Sonifier 450 (50% output, 15 min, 1 sec off, 1 sec on, rest for 1 min in each 5 min) in an ice-water bath, followed by centrifugation (16,000 g, 30 min, 4 °C). The soluble fractions were collected and incubated with pre-equilibrated HisPur™ Ni-NTA Resin (ThermoScientific) (5 mL) at 4 °C for 1 h with constant mechanical rotation. The slurry was loaded onto a Poly-Prep® Chromatography Column, washed with 20 mL of wash buffer (20 mM Tris-HCl pH 8.8,

400 mM NaCl, 20 mM imidazole, 2 mM DTT) for 3 times, and eluted with 3 mL of elution buffer (20 mM Tris-HCl pH 8.8, 400 mM NaCl, 500 mM imidazole, 2 mM DTT) for 5 times. The eluates were concentrated by using Amicon Ultra-15 Centrifugal Filter Devices (30k for LacZ-WT and LacZ-Spy-tag, 3k for spycatcher). The concentrated eluates were buffer exchanged into 3mL of protein storage buffer (20 mM Tris-HCl pH 8.8, 400 mM NaCl, 2 mM DTT, 10% glycerol) using Cytiva PD-10 Sephadex G-25 M desalting columns, and stored at −80 °C after flash freeze for future analysis.

Table 2. Primer information

Primer	Sequences (5' to 3')
LacZ-WT-Nde I-F	aagaaggagatatacatatgaccatgattacggattcactggc
LacZ-LacZ-WT-6xHis-R	caaaacagccaagcttttagtgatggtgatggtgatgtttttgacaccagaccaact
spy-tag-GSlinker-F	tttaagaaggagatatacatatggcgcatatcgtgatggtggatgc
spy-tag-GSlinker-R	ttccggatccacctccggatcctttggtcggtttatacgcatccaccatcacgatatg
pBAD-LacZ-WT-spy-F	gaggtggatccggaagtggtggatccggaagtggatccggaagtatgaccatgattacgg
pBAD-lacz-wt-spy-r	gtatatctccttcttaaagttaaacaaaattatttctagcccaaaaaacgggtatgg
spycatcher-Nde I-F	aagaaggagatatacatatggttgataccttatcaggtttatcaagtgagc
spycatcher-Hind III-6xHis-R	caaaacagccaagcttttagtgatggtgatggtgatgtaaatatgagcgtcacctttag

Gene Blocks information

SpyCatcher:

5’atggttgataccttatcaggtttatcaagtgagcaaggtcagtccggtgatatgacaattgaagaagatagtgctacccat attaaattctcaaaacgtgatgaggacggcaaagagttagctggtgcaactatggagttgcgtgattcatctggtaaaacta ttagtacatggatttcagatggacaagtgaaagatttctacctgtatccaggaaaatatacatttgtcgaaaccgcagcacc agacggttatgaggtagcaactgctattacctttacagttaatgagcaaggtcaggttactgtaaatggcaaagcaactaa aggtgacgctcatattta3’

2.6 Enzyme immobilization

A volume of 200 µL of lactase solution at a concentration of 0.06 mg/ml was dispensed into a Corning 96-well plate, which had been previously coated with a 50 nm layer of polymer with specific chemistry. The plate was then placed in an incubator at 37 °C for 24 hours to facilitate the covalent immobilization of lactase onto the coated surface via amine-epoxide coupling. Direct or site direct immobilization involves an immobilization of Spycatcher, glycine and then finally LacZ-Spytag. Firstly, the immobilization of Spycatcher (0.01 mg), which is like the random immobilization of LacZ-WT followed by a blocking with 1M glycine to get rid of all unreacted epoxide on the immobilization as described by (Gao et al., 2023) and finally the bonding of LacZ-Spytag (0.012 mg) shaking at 30 rpm, 25 °C for 2 hours (C. Li et al., 2021). Following the incubation periods, any residual enzyme solution in the wells was removed, and the wells were rinsed twice with 1× PBS to eliminate any unbound lactase. Immobilized lactases were used immediately for activity and protein quantification.

2.7 Protein Quantification

The protein quantification assay kits, including the Pierce bicinchoninic acid (BCA) assay kit (assay range: 20–2,000 µg/mL) and the Bradford assay kit (assay range: 1–1500 µg/mL) were purchased from ThermoFisher Scientific (Waltham, MA USA).

The quantification of the immobilized lactase was performed using the BCA assay, which generates color upon complexing with protein which is absorbed at a particular wavelength of 562 nm with bovine serum albumin (BSA) utilized as a standard. The immobilization yield (IY) was determined using the formula:

$$IY = \frac{C_i}{C_f} \times 100\%$$

where C_i and C_f denote lactase concentrations (mg/ml) in solution before and after the immobilization, respectively.

2.8 Determination of activity and kinetic parameters

The activity of the surface-free and immobilized lactase was assayed at 37 °C using O-nitrophenyl-beta-D-galactopyranoside (ONPG) as substrate. The ONPG assay was adjusted to specific pH values using 0.1 M phosphate and lactate buffers at different pH values. Immobilized lactases on polymer-coated 96-well plate for each activity test were preheated to the experimental temperature of 37 °C for 10-20 minutes before the addition of substrate solutions. Five (5) different ONPG concentrations from 0 to 16.6 mM in 0.1 M potassium phosphate buffer (pH 6, 7) or lactate buffer (pH 5) were added to the surface-free and immobilized lactases for the conversion of ONPG to *o*-nitrophenol. The change in color developed was measured for 2 minutes at a wavelength of 420 nm using microplate reader (Biotek Synergy H1 MultiMode Microplate Reader w/ Gen 5 Software). A non-linear regression of Michaelis-Menten plot was used to derive kinetic parameters such as Michaelis-Menten constant K_m, turnover number, k_{cat} and catalytic efficiency of lactases.

2.9 Statistical analysis

All treatment and analytical procedures were performed in triplicates (n = 3). Data visualization and statistical analysis were conducted using OriginLab and RStudio, respectively. Analysis of variance (ANOVA) was performed to identify any significant differences among the treatments. Subsequently, a post hoc Tukey's Honest Significant Difference (HSD) test was conducted to identify which specific treatments differed significantly from one another. All statistical analyses were done using significant level of 0.05. Results from Tukey's test were displayed using the compact letter display (CLD).

3.0 Results and Discussion

3.1 Characterization of immobilization supports

The molecular structures of the copolymers (pGE(25), pGB(25), pGD(25), pGD(65), pGDE, and pGDB) as well as the homopolymers (pG, pE, pB, and pD) were confirmed using FTIR spectroscopy (Figure 1). The FTIR spectra of the individual polymers were normalized to their peaks with the highest intensities. Absorption at 910 cm^{-1} was attributed to the characteristic epoxide functional group from the GMA monomer and SAMs of GPTMS. (Sobiesiak, 2019; Vukoje et al., 2014), which plays a crucial role in the covalent immobilization of lactase by providing binding sites for bioconjugation. A weak absorbance around 2770 cm^{-1} corresponds to the tertiary amine group in DMAEMA and SAMs DMAPTMS (Cotanda et al., 2013), which is a key functional group contributing to the polycationic nature of some copolymers (pGD(25), pGD(65), pGDE, and pGDB). The intensity of these functional groups varies with the GMA or DMAEMA content in the copolymers. The absorption at 1730 cm^{-1} is attributed to the carbonyl (C=O) stretch from the methacrylate group, present in all polymers except pB, which does not contain a

methacrylate group. Additionally, in pB and in copolymers crosslinked with DVB, the signal at 820 cm^{-1} corresponds to disubstituted benzene rings. The FTIR confirms the retention of critical function groups like epoxide, which is needed for bioconjugation and the ionizable tertiary amine necessary for modifying the microenvironment of immobilized lactase.

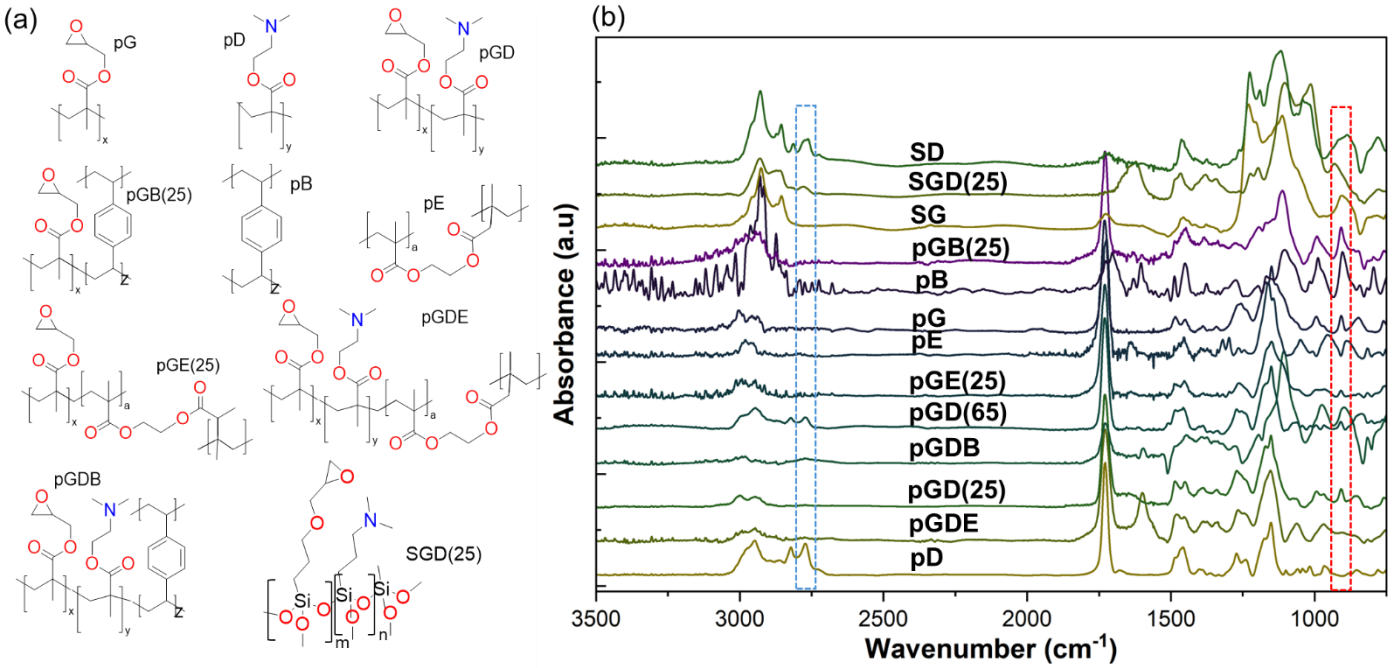

Figure 1. FTIR spectra showing the confirmation of critical functional groups, epoxide (red box) and tertiary amino (blue box), in the synthesized iCVD and SAMs immobilization supports.

3.2 Confirmation of epoxide ring-opening reaction

There are several types of immobilizations, however in our study, our focus was on covalent immobilization as it provides the most stable enzyme-support linkage . To confirm that the immobilization method occurring in our system is covalent immobilization, there must be a reaction (epoxide-amine ring opening) between the epoxide group in the immobilization support and the primary amines on the protein molecule. For this purpose, we performed FTIR characterization of immobilized lactase on pG coated Silicon wafer and pG coated Silicon wafer incubated in 0.1 M phosphate buffer as control. From the

FTIR spectra in (Figure 2), the presence of absorption band at 910 cm^{-1} representing the epoxide group from pG in sample as well as control suggests incomplete utilization of epoxide in sample after lactase immobilization. After lactase immobilization, appearance of peaks around 1640 cm^{-1} and 1550 cm^{-1} was attributed to the bending vibration absorption of NH_2 (amide I) and the deformation vibrations of N-H groups (amide II) (Naeem et al., 2022; Tu et al., 2022) from lactase. In addition, overlapping band between 3200 cm^{-1} and 3600 cm^{-1} was ascribed to N-H stretching vibration at peak position 3300 cm^{-1} and stretching vibrations of OH bond at 3484 cm^{-1} (Naeem et al., 2022; Tu et al., 2022; Vukoje et al., 2014) appeared as a result of epoxide-ring opening reaction in the sample. We then concluded that lactase was attached to the polymer via an epoxide-amine reaction. An additional experiment was performed to block unreacted epoxide function groups with glycine. The spectra for the blocked samples still showed the presence of bands representing epoxide groups as well as bands for amide and hydroxyl functional groups. This suggests an incomplete exhaustion of epoxide groups from the immobilization support. However, due to the 3D structure of iCVD films and the penetration depth (200nm) of IR beam during the FTIR analysis, the signal obtained for the spectra is not just from the surface of the polymer but also from the bulk polymeric structure. As such a different technique such as x-ray photoelectron spectroscopy (XPS) which has a penetration depth of between 5-10 nm can be used for more representative surface chemistry analysis. Interestingly after the blocking with glycine on pG which has no LacZ immobilized, there was no band for OH but a weak band for amide I. This explanation to this may be due to the smaller size of glycine relative to that of LacZ. As

such the more primary amine groups on LacZ contributed more to the epoxide-ring opening reaction to yield more OH groups.

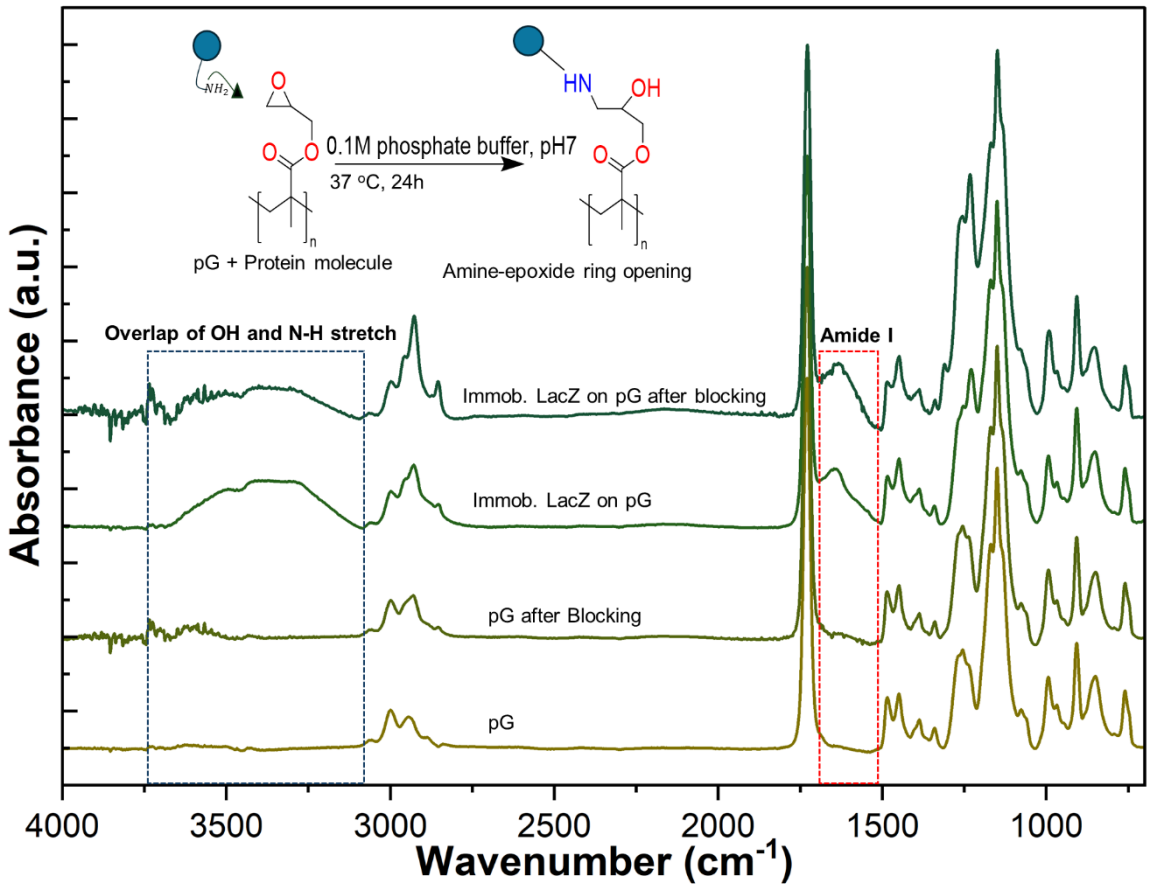

Figure 2. ATR-FTIR spectra showing the confirmation of epoxide ring-opening reaction (covalent immobilization) after lactase immobilization due to the presence of characteristic bands ascribed for amide I (red box) and hydroxyl groups (blue box).

3.3 Impact of direct orientation imposed by bioengineering on the performance of immobilized lactase

Mainly due to the steric hindrance and unwanted interactions between enzymes and immobilization support, the orientation of immobilized enzymes can have a significant impact on the enzyme's activity (Smith et al., 2013). To investigate the impact of immobilized lactase orientation, lactases were immobilized using the traditional random immobilization (RI) system and a direct immobilization (DI) approach through spycatcher/spytag site-specific protein pair system. In both immobilization systems, epoxide functional group in polymer provided the binding site for immobilization where a covalent linkage occurs between the epoxide group and the amine groups of the proteins as in (Figure 3a). We compared the normalized initial rate (v_0^*) as activity of immobilized lactases at pHs 4, 5, 6, 7 and 8 (Figure 3b). There was no detectable activity at pH 4 for either surface free (LacZ-WT and LacZ-ST) or lactase immobilized on pG, regardless of orientation being random (RI, corresponding to LacZ-WT) or controlled (DI, corresponding to LacZ-ST). There was no statistically significant difference in the activities for all lactases at pHs 5 and 6. Upon random immobilization of lactase (LacZ-WT) as in RI-pG (Figure 3b), there was a drastic reduction in activity of lactase at pH 7 and 8. Precisely, there was 92% and 93% reduction in LacZ-WT activity at pH7 and 8, respectively. The reduction in RI-pG activity was due to the negative impact of random immobilization, which is similar to what has been observed in the literature (Barbosa et al., 2015; Kim et al., 2006; Mateo et al., 2007). In addition, the random immobilization approach resulted in a greater amount of lactase immobilized and, consequently, a higher yield compared to the direct immobilization method (Table S4 & S5). This increased yield in random

immobilization was attributed to the abundance of epoxide groups available for bioconjugation with lactase. In contrast, the yield in direct immobilization was constrained by the amount of spycatcher immobilized on the support, less abundant than the available epoxides. It is worth noting that the unnormalized initial rate of both randomly and directedly immobilized lactase are comparable in all treatments. Owing to this, the reduction in randomly immobilized lactase can be attributed to the higher number of lactases on the immobilization support. This was because there was a crowdedness of randomly immobilized lactases causing undesirable enzyme-enzyme interactions, which causes steric hindrance and makes the lactase active site inaccessible to the substrate (Talbert & Goddard, 2012, 2013). This can be delineated from directedly immobilized lactase which had smaller amount of lactase immobilized but yielded higher normalized rate.

However, when lactase (LacZ-ST) was directedly immobilized (DI-pG), there was a retention in activity at pH 7 and an increase in activity at pH 5 (45% increase), pH 6 (57% increase) and pH 8 (20% increase). Comparing randomly and directedly immobilized lactase on pG, there was a significant higher activity in DI for all pH evaluated except pH 4, where no activity was detected in either case. There was about 711% increment in directedly immobilized lactase activity relative to randomly immobilized lactase. This implies that controlling the orientation of immobilized lactase has a significant impact in improving its activity. Conventionally, direct immobilization of lactase increases the rate of conversion of substrates to products.

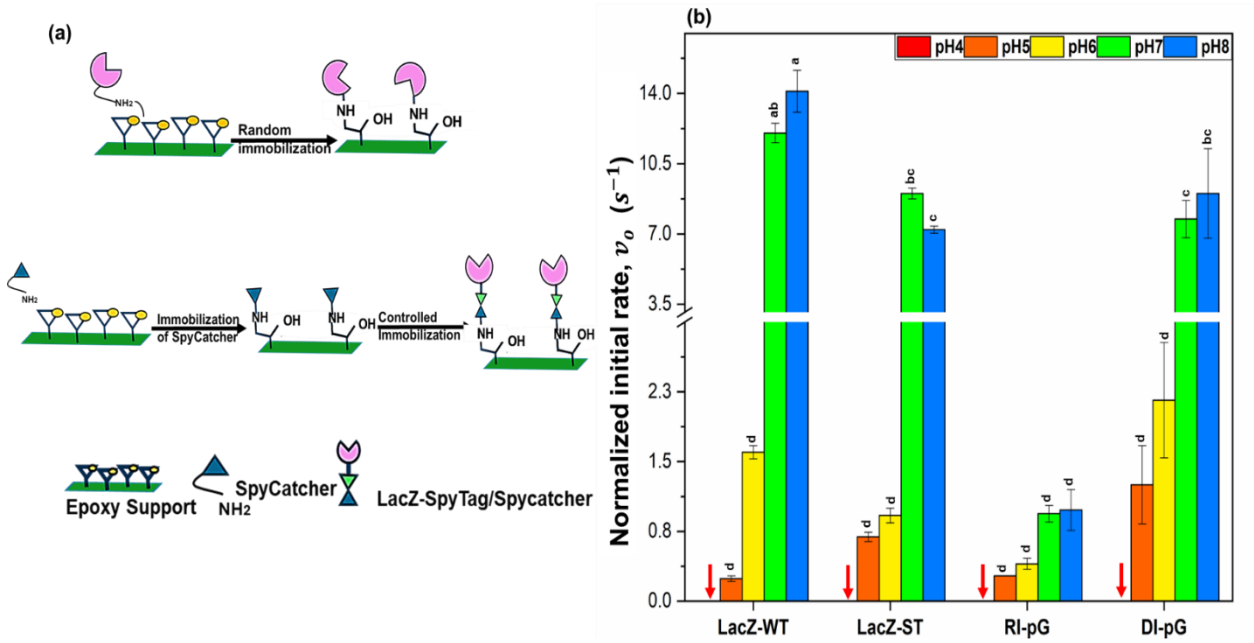

Figure 2. (a) Schematic of direct immobilization (DI) and random immobilization (RI) (b) initial rate of LacZ normalized with its concentration for free LacZ and those immobilized on pGMA (pG) using either random or directed immobilization. Non-overlapping letters denote significant difference, $p < 0.05$. Red arrows: no detectable activity at pH 4.

3.4 Impact of different cross-linkers incorporated in iCVD coatings on the performance of immobilized LacZ

With the major advantage of immobilization being the stability and reusability of the system (Gao et al., 2023; Goddard et al., 2007; Ladero et al., 2001; Mahoney et al., 2013; Smith et al., 2013), we incorporated different crosslinkers into our immobilization supports to enhance mechanical stability and investigate how different crosslinkers affect the activity of immobilized lactases. Crosslinking polymers have been proven in the literature to improve their mechanical properties (Mateo et al., 2007; Mohammadi et al., 2020; Nemani et al., 2018). Furthermore, crosslinkers are known to maintain the integrity of polymer films when exposed to aqueous environments over extended periods of time (Barbosa et al., 2014; Mateo et al., 2007). In addition, the hydrophilicity of crosslinkers in

immobilization support tends to affect some critical properties like conformation that is, 3D spatial arrangement of immobilized biomolecules which may affect the activity of these immobilized molecules (Secundo, 2013). As there is no current data in the literature on how the hydrophilicity of crosslinkers affect the activity of immobilized lactases, a part of our study was to investigate that. We crosslinked the immobilization support with hydrophilic (EGDMA) and hydrophobic (DVB) crosslinkers (see Figure 1a for their structures) and studied the impacts on the activity of both randomly and directedly immobilized lactase. The molar composition of the crosslinker, EGDMA or DVB, was adjusted to be 25% in pGE and pGB, respectively. The composition was confirmed from FTIR quantitative analysis. Again, there was no activity at pH 4 for any of the groups assessed, regardless of orientation and crosslinker type (Figure 4a&b). When the hydrophilic and hydrophobic cross-linked polymers were used as immobilization support for random immobilization (Figure 4a), there was no significant improvement in immobilized lactase activity relative to the lactase immobilized on pG (uncrosslinked polymer). However, in the case of DI (Fig 4b), there was a 264%, 304% and a 96% increase in activity at pH 5, pH 6 and 7, respectively, when the hydrophobic DVB was incorporated in the immobilization support instead of the hydrophilic EGDMA. Comparing DI-pGE(25) and DI-pGB(25), there was an increment of activity about 400% at pH 5, and 640% at pH7 when pGB(25) was used instead of pGE(25). Remarkably, at pH 7, we obtained a 68% increase in LacZ activity on DI-pGB(25) even when compared to the free LacZ-ST. This is very surprising because the immobilization of LacZ almost always leads to a reduction in its activity, rather than a substantial increase (Klein et al., 2018b; Kumar et al., 2009b, 2011; Paiva et al., 2023). Furthermore, LacZ's native environment, cellular

cytosol, is mainly aqueous, and commercial applications, such as lactose removal in liquid milk, also dissolve free LacZ in aqueous solutions. But here we found higher activity on DI-pGB(25), an immobilization support that represents a greater degree of mismatch in hydrophobicity (i.e., surface energy), with LacZ's native aqueous environment. Our result is unexpected because such a mismatch often induces unfavorable protein conformation and even denaturation through hydrophobic interactions (Juers et al., 2012; Secundo, 2013). Notably, such hydrophobicity-induced boosting of activity was only observed with DI, not RI, suggesting that the spycatcher/spytag mediated coupling and/or the site-directed immobilization of the enzymes may be essential to the activity boost.

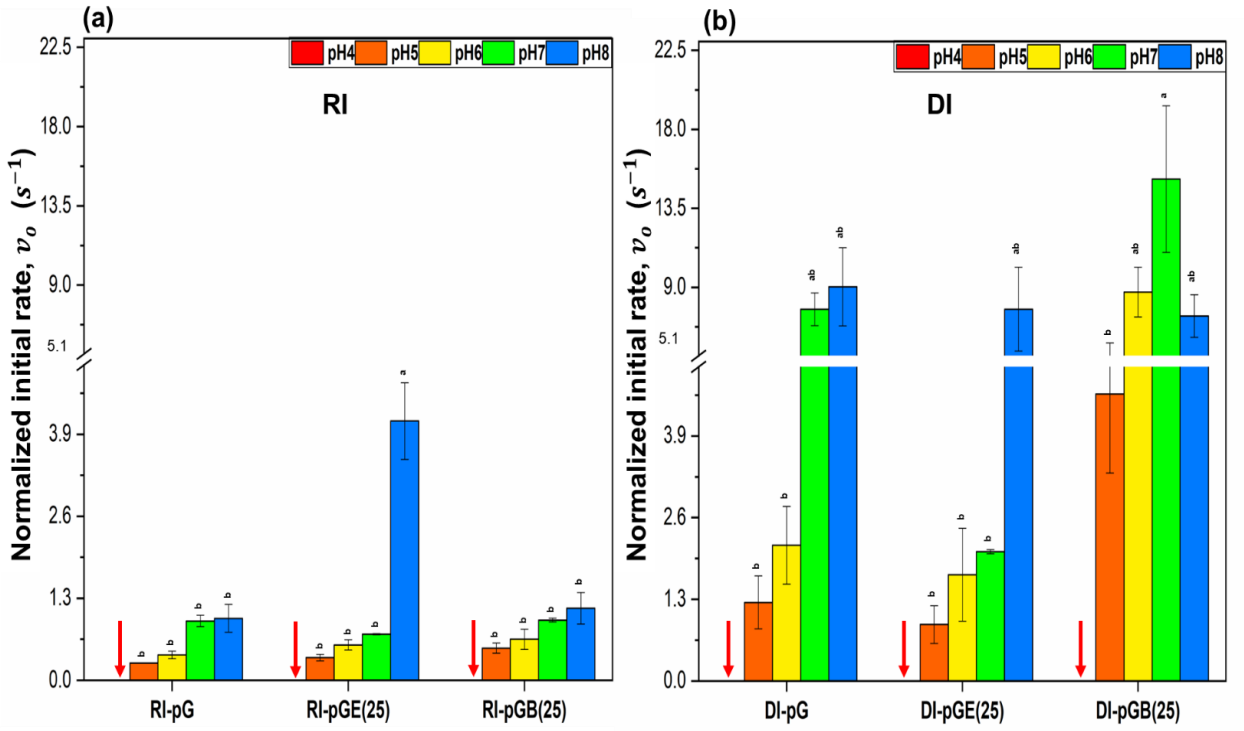

Figure 3. Initial rate of LacZ normalized with its conc. For LacZ immobilized on pGMA (pG), p(GMA-co-25%EGDMA) (pGE(25)) and p(GMA-co-25%DVB) (pGB(25)) using (a) random immobilization (RI) method (b) direct immobilization (DI) method. No detectable activity at pH 4 denoted with red arrows.

3.5 Impact of buffering capacity and ionization of surface moieties on polymeric nanolayers fabricated using iCVD on immobilized lactase activity

Stimuli-responsive polymers, commonly known as "smart" polymers, particularly those responsive to pH changes (André et al., 2005; Dai et al., 2008; Jiang et al., 2006; Wang et al., 2007), have garnered significant attention from researchers. Their ability to create customizable "smart" functional materials has opened the door to a wide range of potential commercial applications, including controlled biological and membrane sciences, drug delivery, personal care products, industrial coatings, oil exploration among others (Dai et al., 2008; Galaev & Mattiasson, 1999; Jeong & Gutowska, 2002; Kost & Langer, 2012; Qiu & Park, 2001; Samal et al., 2012). Reversable protonation of amino

nitrogens in pH lower than their pKa leads to the formation ammonium cations (André et al., 2005; Cotanda et al., 2013; Dai et al., 2008).

To investigate the impact of a pH-responsive on the activity of immobilized at pH 4, a monomer with cationic nature, provided by the presence of tertiary amine groups present in its structure, 2-(N, N-Dimethylamino) ethyl methacrylate (DMAEMA) (Cotanda et al., 2013; Van De Wetering et al., 1999) was incorporated in some copolymers (pGD(25), pGD(65), pGDE and pGDB) used as immobilization support. The molar concentration of DMAEMA in copolymers was estimated by FTIR quantification using Lambert-Beer's law. The effect of the polycationic content in polymeric structure on the activity of immobilized lactases was studied at different pHs. Polymers without DMAEMA were included for comparison. As shown in Fig 5, there was no activity at pH 4 for surface free lactases as well as randomly and directely immobilized lactases on polymers without DMAEMA ("DMAEMA -"Figure 5a&b). In contrast, there was activity at pH 4 for both randomly and directely immobilized lactases on copolymers having the polycationic content provided by DMAEMA ("DMAEMA + "). Considering the pKa (8.4) of tertiary amine group in DMAEMA (Cotanda et al., 2013; Mazied et al., 2009; Van De Wetering et al., 1999), at pH 4, the tertiary amine groups would be the predominantly protonated (>99.99%) according to the Henderson–Hasselbalch equation. The activity observed at pH 4 can be attributed to the formation of ammonium cations providing an electrostatic repulsion against the hydronium ions (H_3O^+) from bulk acidic media of the substrate solution. This electrostatic repulsion creates a shield for the immobilized lactase thus, its immediate local microenvironment is not directely affected by the bulk acid media. Thus, the pH-sensitive amino acid residues on lactase, especially in the active site, such as glutamic acid (pKa

= 3.90), histidine (pKa = 6.04) and lysine (pKa = 10.5) (Becker et al., 2017; Hua et al., 2008) are less affected by the H_3O^+ influx in the acid environment by preventing them from being protonated or deprotonated, which prevents the denaturing or deactivation of lactase. In corroboration of this, we observed that when the concentration of DMAEMA was increased from 25% as in pGD(25) to 65% as in pGD(65) the activity of randomly immobilized lactase at pH 4 increased by 60% (Figure 5a). This can be attributed to the higher concentration of the protonated of DMAEMA, making the ionization process and the electrostatic repulsion more prominent. A similar effect was observed when lactase was directedly immobilized although the activities were higher (DI-pGD25 and DI-pGD(65) (Figure 5b) than in RI (RI-pGD25 and RI-pGD(65) (Figure 5a) at the same pH (pH 4).

When lactase was directedly immobilized on pGDB (a hydrophobic crosslinked copolymer with polycationic content), there was a significant increase in the activity at all pHs (Figure 5b). There was more than 100% increase in activity at suboptimal pHs (4 and 5) and about 540% and 730% increase in activity of immobilized lactase at pH 7 and 8 when the immobilization support used was pGDB instead of pGDE. In addition, the increase in activity of DI-pGDB was still prevalent even comparing it to surface free LacZ, which was above 100% increase at all pHs. The positive impact of hydrophobic crosslinker is evident at all pHs when the pH-responsive functionality was included, strengthening our confidence in the hydrophobicity-induced boosting of LacZ activity. Potential interactions crosslinkers (DVB or EGDMA) and the protonation of DMAEMA are noteworthy. Incorporating a hydrophobic monomer into a copolymer alongside a pH-responsive monomer has been shown to facilitate the protonation of adjacent nitrogens and to reduce

steric hinderance, thus increasing the protonation rate of DMAEMA in the copolymer (Cotanda et al., 2013). The addition of the hydrophobic crosslinker enhanced the electrostatic repulsion observed even at pH 7 and 8, resulting in improved activity for the immobilized lactase.

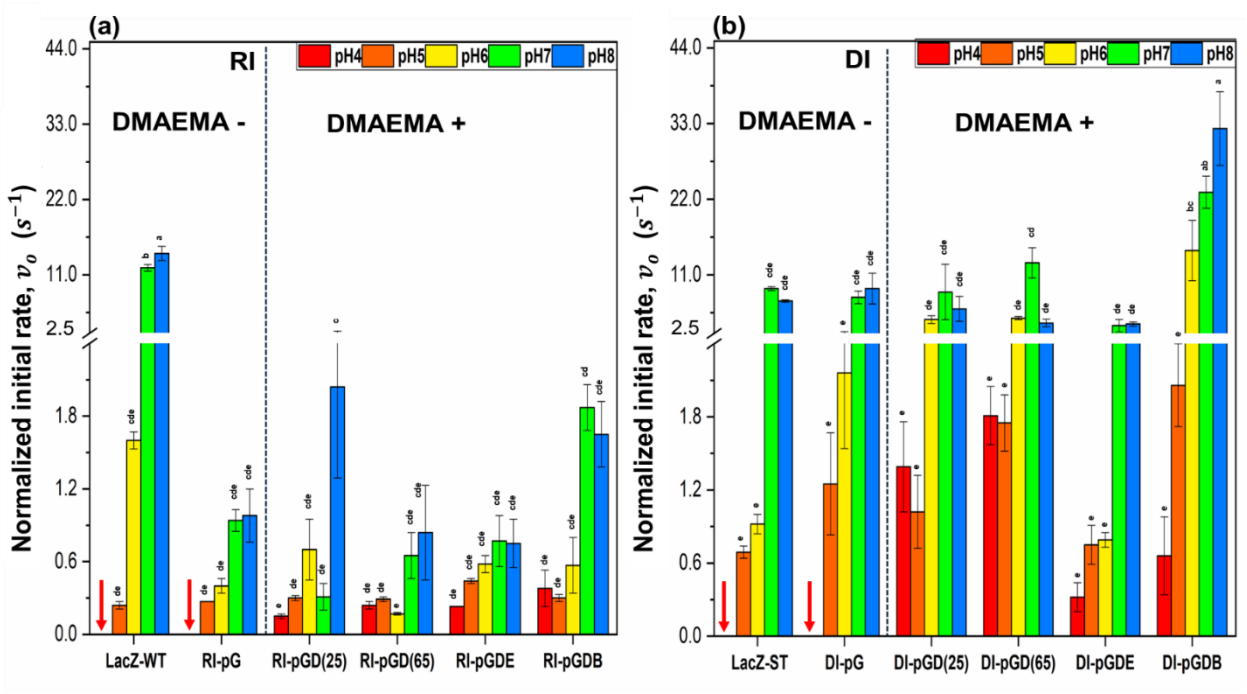

Figure 6. Initial rate of LacZ normalized with its conc. for free LacZ and LacZ immobilized on polymers with and without polycationic content using (a) random immobilization (RI) method (b) direct immobilization (DI) method. No detectable activity at pH 4 denoted with red arrows.

3.6 Assess the impact of employing solution-phase polymerization of Self-Assembly Monolayers (SAMs) as opposed to vapor phase polymerization (iCVD) on the performance of immobilized lactase

An essential factor in regulating protein attachment to supports is the development of surface modification techniques that are substrate-independent and capable of achieving uniform coverage, thereby broadening their applicability across various fields (Yang et al., 2012). The iCVD process is highly versatile, accommodating various materials and geometries, including 3D structures and micro- and nanoscale (Alrifaiy et al., 2012; Teles & Fonseca, 2008). Its ability to create uniform, high-quality films on diverse surfaces, including flexible substrates like 96-well plates and 2D materials for biological applications such as enzyme immobilization (Chen et al., 2016; Gleason, 2015) makes it an excellent choice.

SAM, a solution-phase coating technique, has also been shown to provide versatile enzyme immobilization supports with excellent conformality to substratum materials. The unique organization of silanes on surfaces, extensively studied by the Whitesides group and known as SAMs, offers significant advantages. These surfaces are notable for their rapid synthesis and ease of modification, enabling the presentation of diverse surface chemistries, including homogeneous, mixed, or patterned configurations (Connell et al., 2014; Jones et al., 2008). SAMs have demonstrated immense potential for protein immobilization and other biological applications. Functionalized silane monolayers, especially those utilizing epoxy-silanes and alkyl amines, have gained prominence due to their effectiveness in securely immobilizing biomolecules such as proteins, enzymes, and DNA (Goddard & Hotchkiss, 2007). In this part of our study, we created SAMs with

epoxide, GPTMS and tertiary amine DMAPTMS end groups which are similar to the critical functional groups in the iCVD polymers. These SAMs were used as immobilization support for randomly and directedly immobilized lactase.

We were only able to detect activity at pH 4 for immobilized lactase only on SAMs support with polycationic content similar to what was observed with iCVD polymers. This supports the fact that SAMs also provide the retention of functional groups (Connell et al., 2014; Jones et al., 2008). When the lactase was randomly immobilized (Figure 6c) on SAM there was no significant difference in the activity from lactase immobilized on the iCVD polymers using same immobilization method. This observation was true at all pHs except pH 7 which gave an increase in activity of about 85% when immobilized on SGD(25) instead of pGD(25). After the fabrication of SAMs, the thickness obtained from ellipsometry was 7.4 $\pm$ 0.9 nm while the iCVD film had thickness of 54.0 nm $\pm$ 0.2. In contrast, when lactase was directedly immobilized (Figure 6d) on SAMs, i.e., DI-SGD(25), there was a significant reduction in activity of about 87% at pH 4, 61% at pH5, and 64% at pH7, compared with those immobilized on the corresponding iCVD films, i.e., DI-pGD(25).

When we focus on the activity results at pH 4, where the electrostatic shield effect should be most prominent, we obtain the following findings (see the red arrows and bars in Fig 6c & d). First, the presence of DMAEMA (“D”) in the polymer support was essential to retaining LacZ activity at pH 4, regardless of RI or DI was used, which is consistent with the results presented in Fig 5.

Second, in Fig 6d, when DMAEMA was present, and the DI was used for immobilization, we observed almost 10-fold higher activity at pH 4 (red bards) for LacZ when immobilized

on iCVD films, i.e., DI-pGD(25), than on SAMs, i.e., DI-SGD(25). This can be explained by that, the DI-pGD(25) support, being ~50 nm in thickness, contained more DMAEMA per unit area than the monolayer DI-SGD(25). This greater density of protonatable DMAEMA in turn led to more positively charged functional groups (per unit area) at pH 4 and thereby a stronger electrostatic shield that can protect the active sites from H_3O^+. A similar trend was observed at pH 5 though less prominent.

Third, while the above argument seems reasonable, it was surprising to see that such thickness-dependent improvement was absent at pH 4 or pH 5 when LacZ was randomly immobilized on iCVD films vs SAMs [Fig 6c, RI-pGD(25) vs. RI-SGD(25)]. Note that there was no obvious difference between RI-SGD(25) and DI-SGD(25), but for iCVD films the activity declined sharply (~10-fold lower) from DI-pGD(25) to RI-pGD(25). Thus, we speculate that there may be yet another factor present in the RI of LacZ on pGD(25) that negatively impacted its activity at low pHs. One hypothesis that aligns with these observations is that the flexible polymer chains originating from the iCVD films, due to their wider reach, may hinder ONPG molecules from accessing the active site or interfere with the catalysis reaction within the active site, if the enzymes are randomly oriented; however, the stie-specific immobilization and orientation control achieved through DI enables the enzymes to adopt orientations that mitigate these hinderances. SAMs, on the other hand, are unlikely to extend such polymer to interfere with these processes.

Overall, at pH 4 and 5, directed immobilization of LacZ on multilayered iCVD polycationic films, i.e., DI-pGD(25), achieved a better activity of the immobilized LacZ than achieved on any of the monolayered SAMs supports. A follow-up study is currently underway to compare the stability and reusability of iCVD and SAMs immobilization supports.

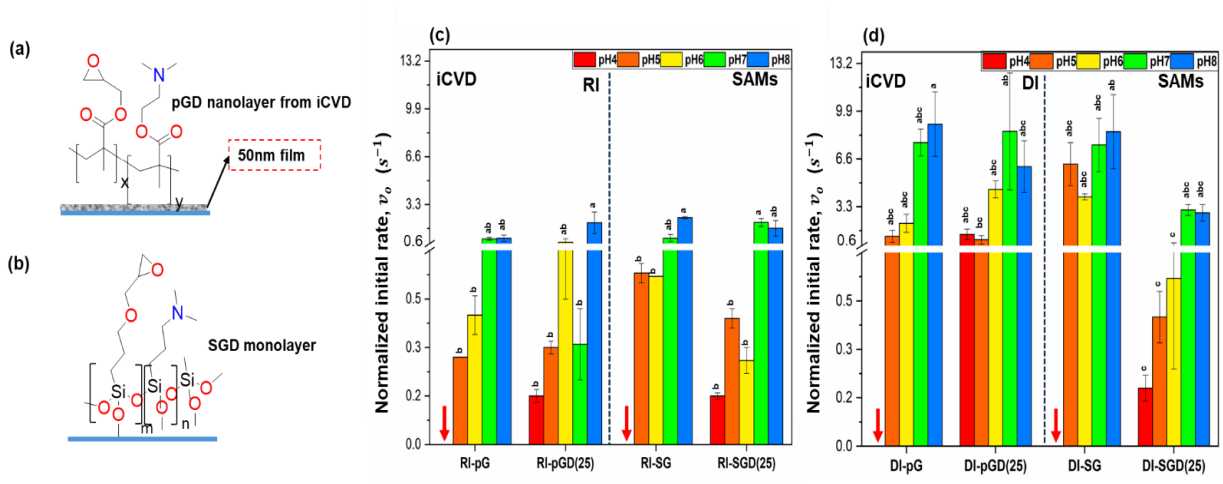

Figure 7. (a) iCVD copolymer of GMA and DMAEMA, (b) SAMs of GPTMS and DMAPTMS, Initial rate of LacZ normalized with its conc. for free LacZ and LacZ immobilized on iCVD polymers and SAMs using (c) random immobilization method (d) direct immobilization method.

3.7 Derived Kinetic parameters surface free and randomly and directedly immobilized lactase

Considering the retention and enhancement of activity of immobilized lactase at a substrate concentration of 16.6 mM ONPG, we examined how kinetic parameters, including K_m, V_{max}, k_{cat} *and* k_{cat} / K_m (catalytic efficiency), were influenced by our immobilization system. Serial dilutions of the 16.6 mM substrate concentration were prepared to establish a range from 0 to 16.6 mM, using either 0.1 M lactate buffer (pH 4) or phosphate buffer (pH 7). The kinetic derived parameters are represented in table 1 and 2 as mean $\pm$ standard error.

While both randomly and directedly immobilized lactase on immobilization with the polycationic content exhibited activity at pH 4, the catalytic efficiencies were lower compared to pH 7. This suggests that optimization is necessary to enhance the cost-

effectiveness of the immobilization system for applications in low-pH waste streams, such as acid whey. Random immobilization of LacZ on all supports led to an apparent increase in K_m and a significant reduction in k_{cat} / K_m. The decrease in catalytic efficiency is likely associated with the increased K_m, indicating reduced binding affinity between the enzyme and substrate, as well as a decrease in k_{cat}. These results align with previous findings for randomly immobilized enzymes, and thus were expected. The calculation of k_{cat} relies on the V_{max} and the protein concentration in the reaction, assuming that all protein present is enzymatically active. A reduction in k_{cat} and catalytic efficiency may be attributed to enzyme denaturation or reorientation on the carrier surface. Inactive enzyme bound to the carrier would result in artificially low turnover numbers and catalytic efficiencies during calculation. This suggests that the loss of activity may stem from increased carrier-protein interactions at the interface (Talbert & Goddard, 2012, 2013; Barbosa et al., 2015; Kim et al., 2006; Mateo et al., 2007). There was an observed increase in K_m and a decrease in catalytic efficiency when lactase was directedly immobilized, despite controlled orientation during immobilization. This contrasts with site-directed immobilization, which typically enhances binding affinity and improves substrate accessibility to the active site (Gao et al., 2023; Smith et al., 2013). Nevertheless, directedly immobilized lactase exhibited higher catalytic efficiency compared to randomly immobilized lactase, although we cannot associate this increase with a reduction in K_m. Both immobilization systems exhibit similar K_m indicating low substrate affinity for ONPG and suggesting that substrate binding is not significantly affected by the immobilization method. The catalytic reaction in both immobilization systems is enzyme-limited rather than diffusion-limited, with catalytic turnover being the rate-determining step. These findings underscore the

importance of optimizing immobilization strategies and microenvironments to enhance catalytic performance in immobilized enzyme systems. Another factor to consider is how the tetrameric structure of lactase influences the coupling of spycatcher and spytag to orient the immobilized enzyme, ensuring that all active sites remain accessible to the substrate. Currently, there is no published research on how the spycatcher/spytag site-directed immobilization system functions with enzymes that naturally exist as tetramers in solution, such as lactase. This highlights the need for further studies to better understand this area. Interestingly, the catalytic efficiency of directedly immobilized lactase on hydrophobic crosslinked copolymers did not retain or improve activity at pH 7, as was observed with the normalized initial rate discussed in sections 3.4 and 3.5, although the turnover numbers are higher and comparable. Among the immobilization supports, directedly immobilized lactase on pGDB (DI-pGDB) gave the highest catalytic efficiency followed by DI-pGD(65) and DI-pGB(25), retaining about 30%, 20% and 17% respectively of the activity of free lactase significantly better than other supports. This highlights again the promising potential of hydrophobic crosslinked copolymers with pH-responsive characteristics, such as pGDB as well as DI-pGB(25), for enhancing or maintaining lactase activity.

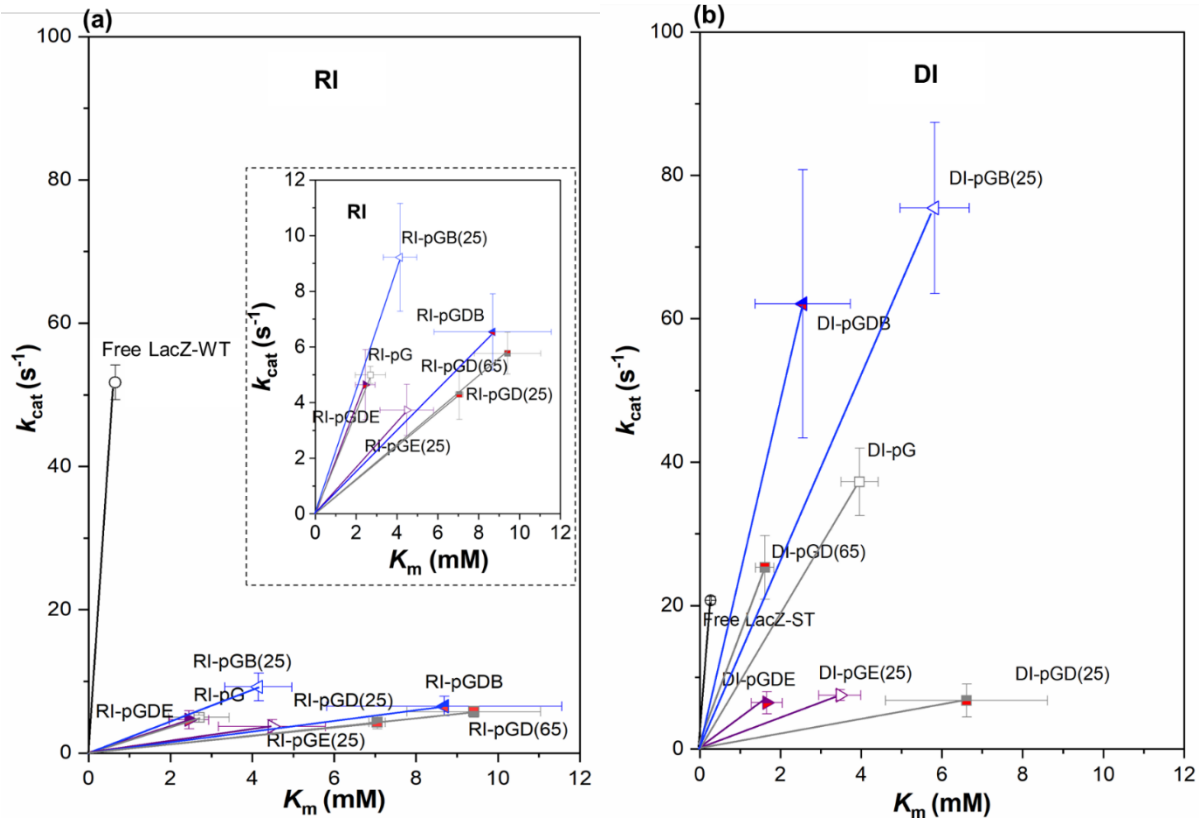

Figure 8. A plot of turnover number against Michaelis constant measured at pH 7 (a) random immobilization method (b) direct immobilization method. The slope of each gives the catalytic efficiency of each LacZ

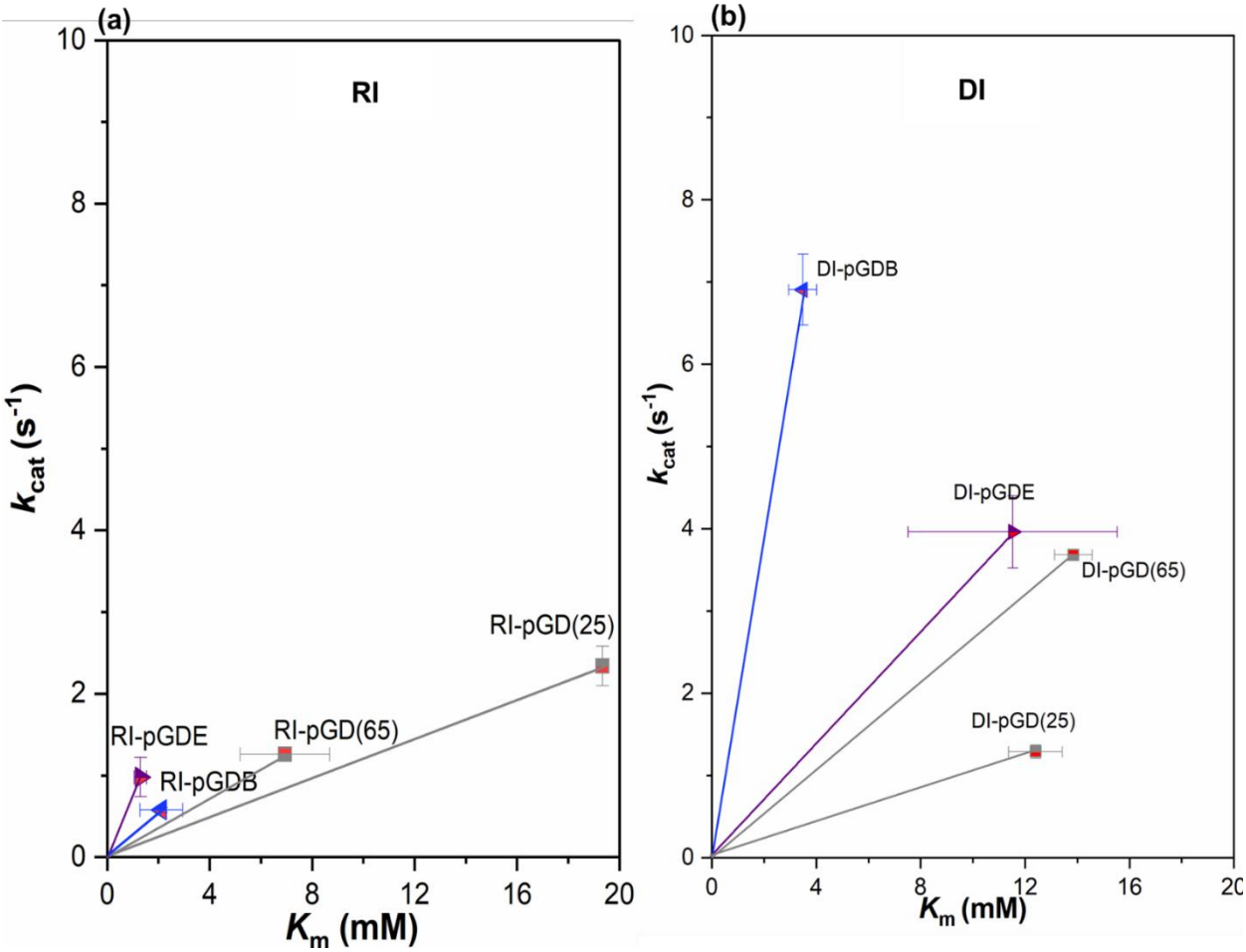

Figure 8. A plot of turnover number against Michaelis constant measured at pH 4 (a) random immobilization method (b) direct immobilization method. The slope of each gives the catalytic efficiency of each LacZ

Table 3. Kinetic Parameters of Randomly Immobilized LacZ-WT at pH 4 & 7 represented as mean ± standard error. Non-overlapping letters represent significant differences.

Microenvironment	pH	V_{max} (mM s^{-1})	K_m (mM)	k_{cat} (s^{-1})	k_{cat}/K_m (mM^{-1} s^{-1})
Surface Free	4	ND	ND	ND	ND
	7	4.48E-03 ± 0.12E-03^{a}	0.67 ± 0.03^{cd}	47.81 ± 1.34^{a}	71.85 ± 4.16^{a}
RI-pG	4	ND	ND	ND	ND
	7	3.85E-05 ± 0.25E-05^{b}	1.82 ± 1.05^{bcd}	5.37 ± 0.35^{bc}	2.10± 0.70^{c}
RI-pGE(25)	4	ND	ND	ND	ND
	7	1.75E-05 ± 0.61E-05^{b}	2.73 ± 1.57^{bcd}	2.75 ± 0.95^{bc}	1.01 ± 0.75^{c}
RI-pGB(25)	4	ND	ND	ND	ND
	7	7.67E-05 ± 1.98E-05^{b}	5.33 ± 1.04^{bcd}	10.37 ± 2.67^{b}	1.95 ± 0.71^{c}
RI-pGD(25)	4	1.51E-05 ± 0.18E-06^{b}	19.33 ± 0.24^{a}	2.34 ± 0.24^{c}	0.12 ± 0.05^{c}
	7	3.23E-05 ± 0.68E-05^{b}	7.05 ± 0.20^{bcd}	4.29 ± 0.90^{bc}	0.61 ± 0.12^{c}
RI-pGD(65)	4	9.37E-06 ± 0.56E-06^{b}	6.94 ± 1.75^{bcd}	1.26 ± 0.07^{c}	0.18 ± 0.06^{c}
	7	4.09E-05 ± 0.68E-05^{b}	14.02 ± 4.06^{b}	5.50 ± 0.91^{bc}	0.39 ± 0.14^{c}
RI-pGDE	4	7.36E-06 ± 1.82E-06^{b}	1.30 ± 0.24^{bcd}	0.98 ± 0.24^{c}	0.75 ± 0.05^{c}
	7	3.50E-05 ± 0.95E-05^{b}	2.45 ± 0.48^{bcd}	4.64 ± 1.26^{bc}	1.89 ± 0.35^{c}
RI-pGDB	4	4.92E-06 ± 0.27E-06^{b}	2.11 ± 0.83^{bcd}	0.58 ± 0.03^{c}	0.27 ± 0.24^{c}
	7	4.01E-05 ± 1.40E-05^{b}	5.11 ± 3.28^{bc}	4.71 ± 1.65^{bc}	0.92 ± 0.66^{c}
RI-SG	4	ND	ND	ND	ND
	7	3.16E-05 ± 1.40E-05^{b}	0.81 ± 0.35^{d}	7.17 ± 1.73^{bc}	8.83 ± 1.32^{b}
RI-SGD(25)	4	4.70E-06 ± 1.28E-06^{b}	3.16 ± 0.79^{bcd}	0.52 ± 0.14^{c}	0.16 ± 0.01^{c}
	7	4.68E-05 ± 0.42E-05^{b}	1.46 ± 0.41^{cd}	5.14 ± 0.46^{bc}	3.53 ± 1.28^{bc}

Table 4. Kinetic Parameters of Directedly Immobilized LacZ-ST at pH 4 & 7 represented as mean ± standard error. Non-overlapping letters represent significant differences.

LacZ Microenvironment	pH	V_{max} (mM s^{-1})	K_m (mM)	k_{cat} (s^{-1})	k_{cat}/K_m (mM^{-1} s^{-1})
Surface Free	4	ND	ND	ND	ND
	7	1.94E-03 ± 0.05E-03^{a}	0.27 ± 0.02^{e}	20.71 ± 0.54^{cd}	75.95 ± 5.13^{a}
DI-pG	4	ND	ND	ND	ND
	7	1.79E-05 ± 0.42E-05^{a}	3.96 ± 0.46^{e}	37.28 ± 4.70^{bc}	9.42 ± 0.08^{c}
DI-pGE(25)	4	ND	ND	ND	ND
	7	5.60E-06±0.57E-06^{b}	3.47 ± 0.52^{e}	7.52 ± 0.77^{cd}	2.17 ± 0.13^{c}
DI-pGB(25)	4	ND	ND	ND	ND
	7	5.61E-05 ± 0.89E-05^{b}	5.82 ±0.86^{cde}	75.46 ± 11.94^{a}	12.97 ± 3.59^{bc}
DI-pGD(25)	4	3.31E-06 ± 0.22E-06^{b}	12.40±1.03^{abc}	1.29 ± 0.08^{d}	0.10 ± 0.00^{c}
	7	1.74E-05 ± 0.58E-05^{b}	6.61 ± 2.01^{bcde}	6.78 ± 2.30^{cd}	1.03 ± 0.35^{c}
DI-pGD(65)	4	1.26E-06 ± 0.13E-06^{b}	13.85±1.25^{ab}	3.68 ± 0.06^{d}	0.27 ± 0.02^{c}
	7	2.23E-05 ± 0.39E-05^{b}	1.61 ± 0.23^{e}	25.31± 4.47^{cd}	15.72 ± 6.11^{bc}
DI-pGDE	4	1.03E-05 ± 0.11E-05^{b}	11.53 ± 4.01^{abcd}	3.96 ± 0.44^{d}	0.34 ± 0.07^{c}
	7	1.65E-05 ± 0.40E-05^{b}	1.66 ± 0.38^{e}	6.45 ± 1.54^{cd}	3.89 ± 0.59^{c}
DI-pGDB	4	5.78E-06 ± 0.36E-06^{b}	3.48 ± 0.54^{e}	6.91 ± 0.43^{cd}	1.98 ± 0.17^{c}
	7	3.37E-05 ± 1.01E-05^{b}	2.55 ± 1.18^{e}	62.09 ±18.70^{ab}	24.32 ± 15.56^{b}
DI-SG	4	ND	ND	ND	ND
	7	1.30E-05 ± 0.01E-05^{b}	5.28 ± 0.55^{cde}	6.80 ± 0.01^{cd}	1.29 ± 0.12^{c}
DI-SGD(25)	4	1.12E-05 ± 0.11E-06^{b}	16.44± 0.07^{a}	6.37 ±0.61^{cd}	0.39 ± 0.04^{c}
	7	2.34E-05 ± 0.72E-05^{b}	4.33 ± 2.33^{de}	13.22 ± 4.05^{cd}	3.06 ± 0.74^{c}

Conclusion

This research presents a multifaceted approach to enhancing immobilized lactase performance through precise control of enzyme orientation and modification of the local microenvironment. The use of iCVD for fabricating tailored polymeric supports, coupled with the Spycatcher/Spytag system for directed immobilization, resulted in significantly improved enzyme activity, particularly at neutral to alkaline pH. The incorporation of hydrophobic crosslinkers further augmented this effect.

A key innovation was the introduction of pH-responsive polycationic moieties into the support structure, enabling lactase activity at pH 4; a condition where the enzyme is typically inactive. This breakthrough expands the potential applications of immobilized lactase in acidic environments, such as those encountered in dairy processing. Our findings underscore the importance of considering both enzyme orientation and local microenvironment in the design of immobilized enzyme systems. This approach opens new avenues for optimizing biocatalyst performance across a wider range of conditions, potentially revolutionizing applications in food processing, biotechnology, and other industries reliant on enzymatic reactions.

Future work should focus on scaling up these systems and exploring their long-term stability and reusability in industrial settings. Additionally, this strategy could be extended to other enzymes, potentially leading to a new generation of highly efficient and versatile immobilized biocatalysts.

Additional experiment

Stability and reusability of immobilized lactases

Given the promising performance of our immobilization system, we conducted a brief experiment to evaluate the stability of our immobilized LacZ. Enhanced stability is a key advantage of enzyme immobilization, enabling enzymes to be reused and easily separated from reaction mixtures (Homaei et al., 2013; D. M. Liu et al., 2018).

The stability of both random and direct immobilized lactases on pG and pGDE were investigated over a period by tracking changes in kinetic parameters over repeated cycles of usage. Immobilized lactases were incubated in 1x PBS at 37 ^{o}C for an hour after each cycle. Activity tests were done following the same methodology as in section 2.8 at various time points (0 -5 hours) during storage of lactases at pH7 and a temperature of 37 ^{o}C. The kinetic parameters for each cycle were derived and used for a plot represented in figure 9 and 10.

The randomly immobilized LacZ exhibited significant fluctuations in immobilized LacZ activity across the reuse cycles Figure 9a and 10a. The initial catalytic efficiency increased dramatically in the first cycle. Subsequent cycles showed variable activity, with the highest value observed in cycle 1 and the lowest in cycle 5 for RI-pG and highest observed in cycle 3 and lowest in cycle 2 as in RI-pGDE. This shows an inconsistent pattern, which suggests that the immobilization method may not provide stable enzyme activity over multiple uses although there was still activity at the 6th cycle. The significant variations between cycles could be attributed to experimental variability, thus the need for the optimization of the experiment. In contrast, directedly immobilized LacZ demonstrated a clearly decreasing trend in LacZ activity over the reuse cycles Figure 9b

and 10b. The initial catalytic efficiency value was substantially higher followed by a sharp decline with 35% for DI-pG and a 40% for DI-pGDE retention of activities in the first cycle. This pattern of decrease in immobilized LacZ activity is more consistent with typical enzyme deactivation profiles observed in immobilized systems. In terms of activity retention over repeated cycles, RI-pG maintained approximately 31% of its initial activity by the 6th cycle, while DI-pG retained only 10%. Despite this, the absolute value of k_{cat} / K_m in cycle 5 was higher for DI-pG than for RI-pG. This suggests that although DI-pG experienced a greater percentage decline, its residual activity remained comparatively stronger. The reduction in activity over repeated cycles is attributable to the possible enzyme leaching as the amount of LacZ immobilized after the 6^{th} cycle is lower than initially quantified Table 4 and 6.

The findings indicate that directed immobilization may improve initial catalytic efficiency but are less effective at maintaining stability over repeated cycles, likely due to enzyme denaturation or leaching from the immobilization matrix. In contrast, the approach used for random immobilization offers greater long-term stability, though it compromises initial activity. However, to maximize enzyme performance across multiple uses, optimization efforts should aim to achieve a balance between high initial activity and sustained reusability. For future experiments, we intend to investigate the stability and reusability of immobilized lactases on the most promising immobilization supports such as the hydrophobic crosslinked polymers (pGB and pGDB) as it was observed in the literature that increased hydrophobicity of the support correlates with enhanced biocatalyst stability. Which was attributed to the reduced water retention of hydrophobic supports, which

minimizes deactivation processes associated with higher hydration levels, thereby helping to preserve the enzyme's structural integrity(Branco et al., 2010).

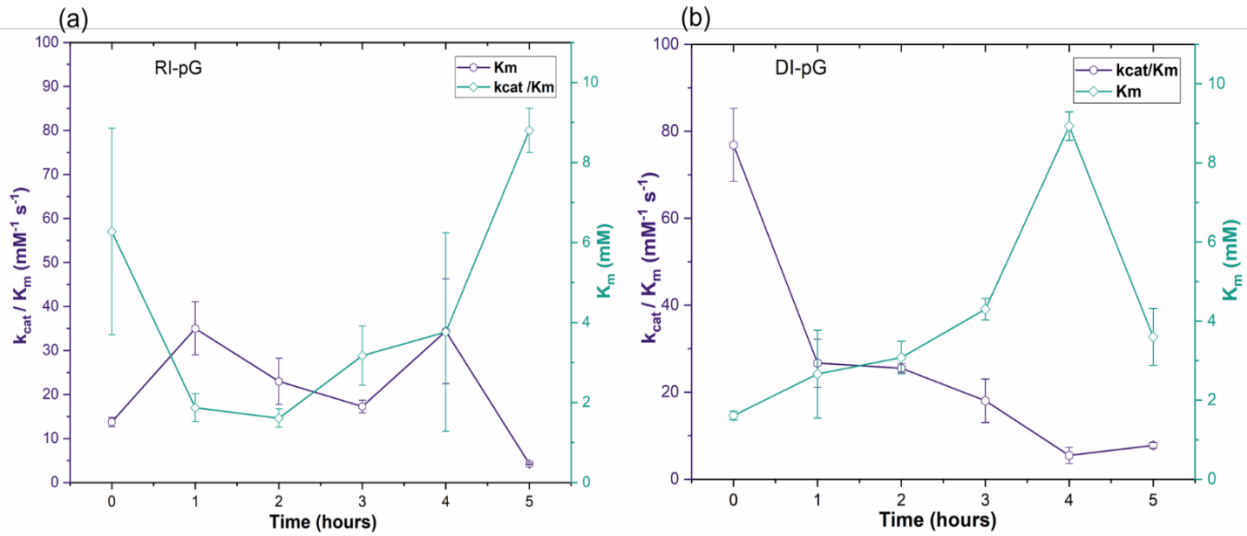

Figure 9. A plot of catalytic efficiency, $k_{\mathrm{cat}}/K_{\mathrm{m}}$ and Michaelis constant, K_{m} measured over repeated cycles of immobilized LacZ on pG (a) random immobilization method (b) direct immobilization method.

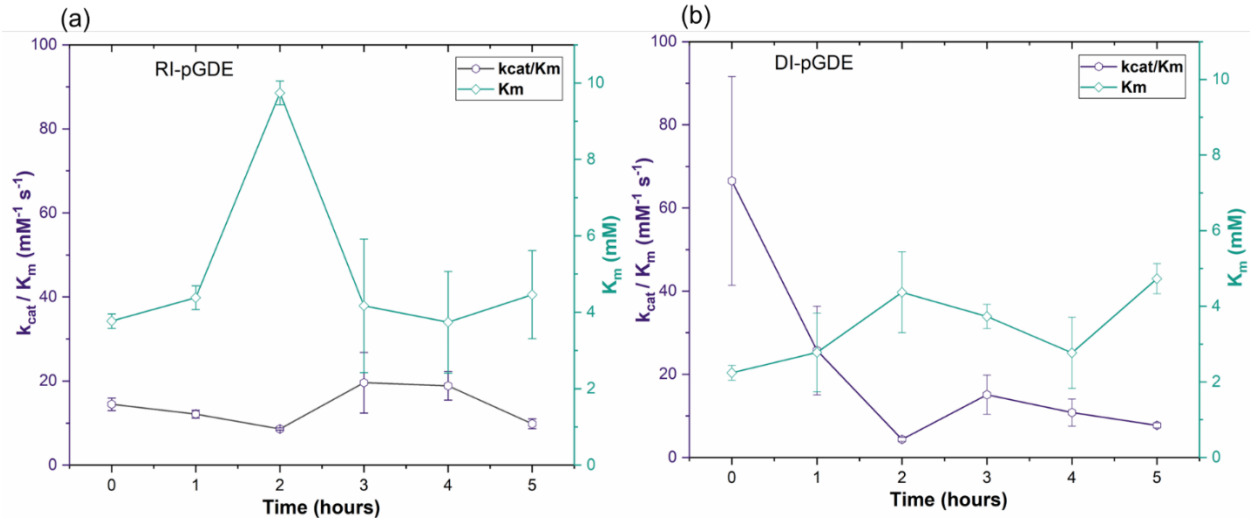

Figure 10. A plot of catalytic efficiency, $k_{\mathrm{cat}}/K_{\mathrm{m}}$ and Michaelis constant, K_{m} measured over repeated cycles of immobilized LacZ on pGDE (a) random immobilization method (b) direct immobilization method.

Table 5. Random Immobilization Yield (IY) after Cycle 1

LacZ Microenvironment	No. LacZ-WT immobilized /100nm^2	IY(%)
RI-pG	60.47 $\pm$ 2.74	10.71 $\pm$ 0.48
RI-pGDE	41.89 $\pm$ 2.06	7.42 $\pm$ 0.36

Table 6. Random Immobilization Yield (IY) after Cycle 6

LacZ Microenvironment	No. LacZ-WT immob. /100nm^2	Yield (%)
RI-pG	54.17 $\pm$ 2.06	9.60 $\pm$ 0.36
RI-pGDE	27.72 $\pm$ 2.58	4.91 $\pm$ 0.46

Table 7. Directed Immobilization Yield (IY) after Cycle 1

LacZ Microenvironment	No. SC immob. /100nm^2	No. LacZ-ST immob. /100nm^2	Percentage of SC occupied by ST(%)	Yield (%)
DI-pG	72.78 $\pm$ 6.89	10.13 $\pm$ 2.85	13.91 $\pm$ 3.91	2.74 $\pm$ 0.77
DI-pGDE	52.48 $\pm$ 1.21	14.57 $\pm$ 2.11	27.76 $\pm$ 4.02	3.95 $\pm$ 0.57

Table 8. Directed Immobilization Yield (IY) after Cycle 6

LacZ Microenvironment	No. SC immob. /100nm^2	No. LacZ-ST immob. /100nm^2	Percentage of SC occupied by ST(%)	Yield (%)
DI-pG	72.78 $\pm$ 6.89	9.63 $\pm$ 0.99	6.75 $\pm$ 0.69	2.61 $\pm$ 0.27
DI-pGDE	52.48 $\pm$ 1.21	10.87 $\pm$ 1.50	20.71 $\pm$ 2.86	2.95 $\pm$ 0.41

References

Alissandratos, A., & Halling, P. J. (2012). Enzymatic acylation of starch. *Bioresource Technology*, *115*. https://doi.org/10.1016/j.biortech.2011.11.030

Alrifaiy, A., Lindahl, O. A., & Ramser, K. (2012). Polymer-based microfluidic devices for pharmacy, biology and tissue engineering. *Polymers*, *4*(3), 1349–1398. https://doi.org/10.3390/polym4031349

Andler, S. M., & Goddard, J. M. (2018). Transforming food waste: how immobilized enzymes can valorize waste streams into revenue streams. In *npj Science of Food* (Vol. 2, Issue 1). Nature Research. https://doi.org/10.1038/s41538-018-0028-2

André, X., Zhang, M., & Müller, A. H. E. (2005). Thermo- and pH-responsive micelles of poly(acrylic acid)-block-poly(N,N- diethylacrylamide). *Macromolecular Rapid Communications*, *26*(7), 558–563. https://doi.org/10.1002/marc.200400510

Ansari, S. A., & Husain, Q. (2012). Potential applications of enzymes immobilized on/in nano materials: A review. In *Biotechnology Advances* (Vol. 30, Issue 3). https://doi.org/10.1016/j.biotechadv.2011.09.005

Asatekin, A., Barr, M. C., Baxamusa, S. H., Lau, K. K. S., Tenhaeff, W., Xu, J., & Gleason, K. K. (2010). Designing polymer surfaces via vapor deposition. In *Materials Today* (Vol. 13, Issue 5). https://doi.org/10.1016/S1369-7021(10)70081-X

Barbosa, O., Ortiz, C., Berenguer-Murcia, Á., Torres, R., Rodrigues, R. C., & Fernandez-Lafuente, R. (2014). Glutaraldehyde in bio-catalysts design: A useful crosslinker and a versatile tool in enzyme immobilization. In *RSC Advances* (Vol. 4, Issue 4, pp. 1583–1600). https://doi.org/10.1039/c3ra45991h

Barbosa, O., Ortiz, C., Berenguer-Murcia, Á., Torres, R., Rodrigues, R. C., & Fernandez-Lafuente, R. (2015). Strategies for the one-step immobilization-purification of enzymes as industrial biocatalysts. In *Biotechnology Advances* (Vol. 33, Issue 5). https://doi.org/10.1016/j.biotechadv.2015.03.006

Becker, S. A., Feist, A. M., Mo, M. L., Hannum, G., Palsson, B. Ø. |[Oslash]| O., Herrgard, M. J., Mäkelä, J., Kandavalli, V., Ribeiro, A. S., Fell, D. A., Wagner, A., Robinson, A., van Oijen, A. M., Higgins, N. P., Hubin, E. A., Fay, A., Xu, C., Bean, J. M., Saecker, R. M., … Owczarzy, R. (2017). Greek yogurt's biggest guns explore creative ways to address acid whey challenge. *Science*. https://doi.org/10.1016/j.ymben.2014.05.014

Branco, R. V., Estrada Gutarra, M. L., Freire, D. M. G., & Almeida, R. V. (2010). Immobilization and characterization of a recombinant thermostable lipase (Pf2001) from pyrococcus furiosus on supports with different degrees of hydrophobicity. *Enzyme Research*, *2010*. https://doi.org/10.4061/2010/180418

Bylund, G. (2015). The Chemestry of Milk - Dairy Processing Handbook. In *Tetra Pak Processing Systems* (Vol. G3).

Celentano, W., Neri, G., Distante, F., Li, M., Messa, P., Chirizzi, C., Chaabane, L., De Campo, F., Metrangolo, P., Baldelli Bombelli, F., & Cellesi, F. (2020). Design of fluorinated hyperbranched polyether copolymers for 19F MRI nanotheranostics. *Polymer Chemistry*, *11*(24). https://doi.org/10.1039/d0py00393j

Chandrapala, J., Duke, M. C., Gray, S. R., Weeks, M., Palmer, M., & Vasiljevic, T. (2016). Nanofiltration and nanodiafiltration of acid whey as a function of pH and temperature. *Separation and Purification Technology*, *160*. https://doi.org/10.1016/j.seppur.2015.12.046

Chen, N., Kim, D. H., Kovacik, P., Sojoudi, H., Wang, M., & Gleason, K. K. (2016). Polymer Thin Films and Surface Modification by Chemical Vapor Deposition: Recent Progress. In *Annual Review of Chemical and Biomolecular Engineering* (Vol. 7). https://doi.org/10.1146/annurev-chembioeng-080615-033524

CHIBATA, I. (1979). *Immobilized Microbial Cells with Polyacrylamide Gel and Carrageenan and Their Industrial Applications*. https://doi.org/10.1021/bk-1979-0106.ch013

Coclite, A. M., Howden, R. M., Borrelli, D. C., Petruczok, C. D., Yang, R., Yagüe, J. L., Ugur, A., Chen, N., Lee, S., Jo, W. J., Liu, A., Wang, X., & Gleason, K. K. (2013). 25th Anniversary Article: CVD polymers: A new paradigm for surface modification and device fabrication. In *Advanced Materials* (Vol. 25, Issue 38). https://doi.org/10.1002/adma.201301878

Connell, L. S., Romer, F., Suárez, M., Valliant, E. M., Zhang, Z., Lee, P. D., Smith, M. E., Hanna, J. V., & Jones, J. R. (2014). Chemical characterisation and fabrication of chitosan-silica hybrid scaffolds with 3-glycidoxypropyl trimethoxysilane. *Journal of Materials Chemistry B*, *2*(6), 668–680. https://doi.org/10.1039/c3tb21507e

Cotanda, P., Wright, D. B., Tyler, M., & O'Reilly, R. K. (2013). A comparative study of the stimuli-responsive properties of DMAEA and DMAEMA containing polymers. *Journal of Polymer Science, Part A: Polymer Chemistry*, *51*(16), 3333–3338. https://doi.org/10.1002/pola.26730

Cruz Sanchez, F. A., Boudaoud, H., Hoppe, S., & Camargo, M. (2017). Polymer recycling in an open-source additive manufacturing context: Mechanical issues. *Additive Manufacturing*, *17*. https://doi.org/10.1016/j.addma.2017.05.013

Dai, S., Ravi, P., & Tam, K. C. (2008). pH-Responsive polymers: Synthesis, properties and applications. *Soft Matter*, *4*(3), 435–449. https://doi.org/10.1039/b714741d

Das, B., Sarkar, S., Maiti, S., & Bhattacharjee, S. (2016). Studies on production of ethanol from cheese whey using Kluyveromyces marxianus. *Materials Today: Proceedings*, *3*(10). https://doi.org/10.1016/j.matpr.2016.10.006

Datta, S., Christena, L. R., & Rajaram, Y. R. S. (2013). Enzyme immobilization: an overview on techniques and support materials. *3 Biotech*, *3*(1), 1–9. https://doi.org/10.1007/s13205-012-0071-7

de Bruin, A. (2018). “Surface Treatments for Biological, Chemical and Physical Applications.” *Johnson Matthey Technology Review*, *62*(3). https://doi.org/10.1595/205651318x696873

Decher, Gero., & Schlenoff, J. B. (2012). *Multilayer Thin Films : Sequential Assembly of Nanocomposite Materials.* Wiley.

dos Santos, J. C. S., Rueda, N., Gonçalves, L. R. B., & Fernandez-Lafuente, R. (2015). Tuning the catalytic properties of lipases immobilized on divinylsulfone activated agarose by altering its nanoenvironment. *Enzyme and Microbial Technology*, *77*. https://doi.org/10.1016/j.enzmictec.2015.05.001

Erickson, B. (2017). Acid whey: Is the waste product and untapped goldmine? *Chemical Engineering News*, *95*(6).

F. F. Freitas, L. D. S. Marquez, G. P. Ribeiro, G. C. Brandao, V. L. Cardoso, & E. J. Ribeiro. (2012). immobilization paper. *Brazilian Journal of Chemical Engineering*, *29*, 15–24.

Fang, J. M., Fowler, P. A., Tomkinson, J., & Hill, C. A. S. (2002). The preparation and characterisation of a series of chemically modified potato starches. *Carbohydrate Polymers*, *47*(3). https://doi.org/10.1016/S0144-8617(01)00187-4

Faucheux, N., Schweiss, R., Lützow, K., Werner, C., & Groth, T. (2004). Self-assembled monolayers with different terminating groups as model substrates for cell adhesion studies. *Biomaterials*, *25*(14), 2721–2730. https://doi.org/10.1016/j.biomaterials.2003.09.069

Friedel, M., Baumketner, A., & Shea, J. E. (2007). Stability of a protein tethered to a surface. *Journal of Chemical Physics*, *126*(9). https://doi.org/10.1063/1.2464114

Galaev, I. Y., & Mattiasson, B. (1999). ‘Smart’ polymers and what they could do in biotechnology and medicine. *Trends in Biotechnology*, *17*(8), 335–340. https://doi.org/10.1016/S0167-7799(99)01345-1

Gao, X., Wei, C., Qi, H., Li, C., Lu, F., & Qin, H. M. (2023). Directional immobilization of D-allulose 3-epimerase using SpyTag/SpyCatcher strategy as a robust biocatalyst for synthesizing D-allulose. *Food Chemistry*, *401*. https://doi.org/10.1016/j.foodchem.2022.134199

Giovannucci, D., Scherr, S. J., Nierenberg, D., Hebebrand, C., Shapiro, J., Milder, J., & Wheeler, K. (2012). Food and Agriculture: The Future of Sustainability. *SSRN Electronic Journal*. https://doi.org/10.2139/ssrn.2054838

Gleason, K. K. (2015). CVD Polymers: Fabrication of Organic Surfaces and Devices. In *CVD Polymers: Fabrication of Organic Surfaces and Devices*. https://doi.org/10.1002/9783527690275

Gleason, K. K. (2019). Organic surface functionalization by initiated CVD (iCVD). In *Surface Modification of Polymers: Methods and Applications* (pp. 107–134). wiley. https://doi.org/10.1002/9783527819249.ch4

Goddard, J. M., & Hotchkiss, J. H. (2007). Polymer surface modification for the attachment of bioactive compounds. In *Progress in Polymer Science (Oxford)* (Vol. 32, Issue 7, pp. 698–725). https://doi.org/10.1016/j.progpolymsci.2007.04.002

Goddard, J. M., Talbert, J. N., & Hotchkiss, J. H. (2007). Covalent attachment of lactase to low-density polyethylene films. *Journal of Food Science*, *72*(1), E036–E041. https://doi.org/10.1111/j.1750-3841.2006.00203.x

Godfray, H. C. J., Beddington, J. R., Crute, I. R., Haddad, L., Lawrence, D., Muir, J. F., Pretty, J., Robinson, S., Thomas, S. M., & Toulmin, C. (2010). Food security: The challenge of feeding 9 billion people. In *Science* (Vol. 327, Issue 5967). https://doi.org/10.1126/science.1185383

Guimarães, P. M. R., Teixeira, J. A., & Domingues, L. (2010). Fermentation of lactose to bio-ethanol by yeasts as part of integrated solutions for the valorisation of cheese whey. In *Biotechnology Advances* (Vol. 28, Issue 3). https://doi.org/10.1016/j.biotechadv.2010.02.002

Gürsoy, M. (2021). Vapor deposition polymerization of synthetic rubber thin film in a plasma enhanced chemical vapor deposition reactor. *Journal of Applied Polymer Science*, *138*(4). https://doi.org/10.1002/app.49722

Hernandez, K., & Fernandez-Lafuente, R. (2011). Control of protein immobilization: Coupling immobilization and site-directed mutagenesis to improve biocatalyst or biosensor performance. In *Enzyme and Microbial Technology* (Vol. 48, Issue 2, pp. 107–122). https://doi.org/10.1016/j.enzmictec.2010.10.003

Homaei, A. A., Sariri, R., Vianello, F., & Stevanato, R. (2013). Enzyme immobilization: An update. In *Journal of Chemical Biology* (Vol. 6, Issue 4, pp. 185–205). Springer Verlag. https://doi.org/10.1007/s12154-013-0102-9

Hua, L., Zhou, R., Thirumalai C, D., & Berne, B. J. (2008). Urea denaturation by stronger dispersion interactions with proteins than water implies a 2-stage unfolding. *Proceedings of the National Academy of Sciences of the United States of America*, *105*(44). https://doi.org/10.1073/pnas.0808427105

Im, S. G., Kim, B. S., Tenhaeff, W. E., Hammond, P. T., & Gleason, K. K. (2009). A directly patternable click-active polymer film via initiated chemical vapor deposition (iCVD). *Thin Solid Films*, *517*(12), 3606–3611. https://doi.org/10.1016/j.tsf.2009.01.040

Immobilization of Enzymes and Cells SECOND EDITION. (n.d.).

Jeong, B., & Gutowska, A. (2002). Lessons from nature: stimuli-responsive polymers and their biomedical applications. *Trends in Biotechnology*, *20*(7), 305–311. https://doi.org/10.1016/S0167-7799(02)01962-5

Jones, J. A., Qin, L. A., Meyerson, H., Il, K. K., Matsuda, T., & Anderson, J. M. (2008). Instability of self-assembled monolayers as a model material system for macrophage/FBGC cellular behavior. *Journal of Biomedical Materials Research - Part A*, *86*(1), 261–268. https://doi.org/10.1002/jbm.a.31660

Juers, D. H., Matthews, B. W., & Huber, R. E. (2012). LacZ β-galactosidase: Structure and function of an enzyme of historical and molecular biological importance. In *Protein Science* (Vol. 21, Issue 12, pp. 1792–1807). https://doi.org/10.1002/pro.2165

Kalia, J., Abbott, N. L., & Raines, R. T. (2007). General method for site-specific protein immobilization by staudinger ligation. *Bioconjugate Chemistry*, *18*(4). https://doi.org/10.1021/bc0603034

Ketterings, Q. , K. C. S. C. G. G. and K. Ganoe. (2017). *Guidelines for Land Application of Acid Whey.* http://nmsp.cals.cornell.edu/publications/files/AcidWheyGuidelines2017.pdf

Khlyustova, A., Cheng, Y., & Yang, R. (2020a). Vapor-deposited functional polymer thin films in biological applications. In *Journal of Materials Chemistry B* (Vol. 8, Issue 31, pp. 6588–6609). Royal Society of Chemistry. https://doi.org/10.1039/d0tb00681e

Khlyustova, A., Cheng, Y., & Yang, R. (2020b). Vapor-deposited functional polymer thin films in biological applications. In *Journal of Materials Chemistry B* (Vol. 8, Issue 31, pp. 6588–6609). Royal Society of Chemistry. https://doi.org/10.1039/d0tb00681e

Khoo, Y. S., Lau, W. J., Liang, Y. Y., Karaman, M., Gürsoy, M., & Ismail, A. F. (2020). A green approach to modify surface properties of polyamide thin film composite membrane for improved antifouling resistance. *Separation and Purification Technology*, *250*. https://doi.org/10.1016/j.seppur.2020.116976

Kierstan, M. P., & Coughlan, M. P. (1991). Immobilization of proteins by noncovalent procedures: principles and applications. In *Bioprocess technology* (Vol. 14).

Kim, J., Grate, J. W., & Wang, P. (2006). Nanostructures for enzyme stabilization. *Chemical Engineering Science*, *61*(3), 1017–1026. https://doi.org/10.1016/j.ces.2005.05.067

Klein, M. P., Sant'Ana, V., Hertz, P. F., Rodrigues, R. C., & Ninow, J. L. (2018a). Kinetics and thermodynamics of thermal inactivation of β-galactosidase from

Aspergillus oryzae. *Brazilian Archives of Biology and Technology*, *61*. https://doi.org/10.1590/1678-4324-2018160489

Klein, M. P., Sant'Ana, V., Hertz, P. F., Rodrigues, R. C., & Ninow, J. L. (2018b). Kinetics and thermodynamics of thermal inactivation of β-galactosidase from Aspergillus oryzae. *Brazilian Archives of Biology and Technology*, *61*. https://doi.org/10.1590/1678-4324-2018160489

Kost, J., & Langer, R. (2012). Responsive polymeric delivery systems. *Advanced Drug Delivery Reviews*, *64*(SUPPL.), 327–341. https://doi.org/10.1016/J.ADDR.2012.09.014

Kumar, S., Dwevedi, A., & Kayastha, A. M. (2009a). Immobilization of soybean (Glycine max) urease on alginate and chitosan beads showing improved stability: Analytical applications. *Journal of Molecular Catalysis B: Enzymatic*, *58*(1–4), 138–145. https://doi.org/10.1016/j.molcatb.2008.12.006

Kumar, S., Dwevedi, A., & Kayastha, A. M. (2009b). Immobilization of soybean (Glycine max) urease on alginate and chitosan beads showing improved stability: Analytical applications. *Journal of Molecular Catalysis B: Enzymatic*, *58*(1–4), 138–145. https://doi.org/10.1016/j.molcatb.2008.12.006

Kumar, S., Singh, J., Agrawal, V. V., Ahamad, M., & Malhotra, B. D. (2011). Biocompatible self-assembled monolayer platform based on (3-glycidoxypropyl)trimethoxysilane for total cholesterol estimation. *Analytical Methods*, *3*(10), 2237–2245. https://doi.org/10.1039/c1ay05231d

La Mantia, F. P., Ceraulo, M., Testa, P., & Morreale, M. (2021). Biodegradable polymers for the production of nets for agricultural product packaging. *Materials*, *14*(2). https://doi.org/10.3390/ma14020323

Ladero, M., Santos, A., García, J. L., & García-Ochoa, F. (2001). Activity over lactose and ONPG of a genetically engineered β-galactosidase from Escherichia coli in solution and immobilized: Kinetic modelling. *Enzyme and Microbial Technology*, *29*(2–3). https://doi.org/10.1016/S0141-0229(01)00366-0

Li, C., Li, L., Feng, Z., Guan, L., Lu, F., & Qin, H. M. (2021). Two-step biosynthesis of D-allulose via a multienzyme cascade for the bioconversion of fruit juices. *Food Chemistry*, *357*. https://doi.org/10.1016/j.foodchem.2021.129746

Li, L., Fierer, J. O., Rapoport, T. A., & Howarth, M. (2014). Structural analysis and optimization of the covalent association between SpyCatcher and a peptide tag. *Journal of Molecular Biology*, *426*(2), 309–317. https://doi.org/10.1016/j.jmb.2013.10.021

Lievore, P., Simões, D. R. S., Silva, K. M., Drunkler, N. L., Barana, A. C., Nogueira, A., & Demiate, I. M. (2015). Chemical characterisation and application of acid whey in

fermented milk. *Journal of Food Science and Technology*, *52*(4). https://doi.org/10.1007/s13197-013-1244-z

Lim, S. I., Mizuta, Y., Takasu, A., Kim, Y. H., & Kwon, I. (2014). Site-specific bioconjugation of a murine dihydrofolate reductase enzyme by copper(I)-catalyzed azide-alkyne cycloaddition with retained activity. *PLoS ONE*, *9*(6). https://doi.org/10.1371/journal.pone.0098403

Liu, D. M., Chen, J., & Shi, Y. P. (2018). Advances on methods and easy separated support materials for enzymes immobilization. In *TrAC - Trends in Analytical Chemistry* (Vol. 102). https://doi.org/10.1016/j.trac.2018.03.011

Liu, G. Y., Sun, W. F., & Lei, Q. Q. (2021). Charge injection and dielectric characteristics of polyethylene terephthalate based on semiconductor electrodes. *Materials*, *14*(6). https://doi.org/10.3390/ma14061344

M. Subramaniam, P. G. W. L. A. I. M. G. (2019). *Synthetic of Polydivinylbenzene Block Hyperbranched Polyethylene Copolymers via Atom Transfer Radical Polymerization*. https://doi.org/10.30919/esmm5f

Mahoney, K. W., Talbert, J. N., & Goddard, J. M. (2013). Effect of polyethylene glycol tether size and chemistry on the attachment of lactase to polyethylene films. *Journal of Applied Polymer Science*, *127*(2), 1203–1210. https://doi.org/10.1002/app.37622

Marć, M., Bystrzanowska, M., Pokajewicz, K., & Tobiszewski, M. (2021). Multivariate assessment of procedures for molecularly imprinted polymer synthesis for pesticides determination in environmental and agricultural samples. *Materials*, *14*(22). https://doi.org/10.3390/ma14227078

Martin, T. P., Lau, K. K. S., Chan, K., Mao, Y., Gupta, M., Shannan O'Shaughnessy, W., & Gleason, K. K. (2007). Initiated chemical vapor deposition (iCVD) of polymeric nanocoatings. *Surface and Coatings Technology*, *201*(22-23 SPEC. ISS.), 9400–9405. https://doi.org/10.1016/j.surfcoat.2007.05.003

Mateo, C., Palomo, J. M., Fernandez-Lorente, G., Guisan, J. M., & Fernandez-Lafuente, R. (2007). Improvement of enzyme activity, stability and selectivity via immobilization techniques. In *Enzyme and Microbial Technology* (Vol. 40, Issue 6, pp. 1451–1463). https://doi.org/10.1016/j.enzmictec.2007.01.018

Mazied, N. A., Ismail, S. A., & Abou Taleb, M. F. (2009). Radiation synthesis of poly[(dimethylaminoethyl methacrylate)-co-(ethyleneglycol dimethacrylate)] hydrogels and its application as a carrier for anticancer delivery. *Radiation Physics and Chemistry*, *78*(11), 899–905. https://doi.org/10.1016/j.radphyschem.2009.06.016

Menchik, P., Zuber, T., Zuber, A., & Moraru, C. I. (2019). Short communication: Composition of coproduct streams from dairy processing: Acid whey and milk permeate. *Journal of Dairy Science*, *102*(5). https://doi.org/10.3168/jds.2018-15951

Mintel. (2019). *Yogurt and Yogurt Drinks—US—November 2019.* https://store.mintel.com/yogurt-and-yogurt-drinks-us-november-2019

Mohammadi, N. S., Khiabani, M. S., Ghanbarzadeh, B., & Mokarram, R. R. (2020). Improvement of lipase biochemical properties via a two-step immobilization method: Adsorption onto silicon dioxide nanoparticles and entrapment in a polyvinyl alcohol/alginate hydrogel. *Journal of Biotechnology*, *323*, 189–202. https://doi.org/10.1016/J.JBIOTEC.2020.07.002

N. Marı´-Buye´, S. O. C. C. C. E. S. K. K. G. and S. B. (2009). *Organic and Hybrid Photonic Crystals*.

Naeem, A., Yu, C., Zhu, W., Chen, X., Wu, X., Chen, L., Zang, Z., & Guan, Y. (2022). Gallic Acid-Loaded Sodium Alginate-Based (Polyvinyl Alcohol-Co-Acrylic Acid) Hydrogel Membranes for Cutaneous Wound Healing: Synthesis and Characterization. *Molecules*, *27*(23). https://doi.org/10.3390/molecules27238397

Nemani, S. K., Annavarapu, R. K., Mohammadian, B., Raiyan, A., Heil, J., Haque, Md. A., Abdelaal, A., & Sojoudi, H. (2018). Surface Modification: Surface Modification of Polymers: Methods and Applications (Adv. Mater. Interfaces 24/2018). *Advanced Materials Interfaces*, *5*(24). https://doi.org/10.1002/admi.201870121

Ng, Z. C., Roslan, R. A., Lau, W. J., Gürsoy, M., Karaman, M., Jullok, N., & Ismail, A. F. (2020). A green approach to modify surface properties of polyurethane foam for enhanced oil absorption. *Polymers*, *12*(9). https://doi.org/10.3390/POLYM12091883

Paiva, M., Paula-Elias, F., Pereira, L., Carreiro, S., Vieira-Almeida, E., Silva, E., Dias, G., Xavier, M., Morales, S., Perna, R., & Almeida, A. (2023). Stabilization of β-Galactosidase Encapsulated in Pectin-Alginate Hydrogel and Hydrolysis of Whey Lactose and Whole Milk. *Journal of the Brazilian Chemical Society*. https://doi.org/10.21577/0103-5053.20230067

Qiu, Y., & Park, K. (2001). Environment-sensitive hydrogels for drug delivery. *Advanced Drug Delivery Reviews*, *53*(3), 321–339. https://doi.org/10.1016/S0169-409X(01)00203-4

Rocha-Mendoza, D., Kosmerl, E., Krentz, A., Zhang, L., Badiger, S., Miyagusuku-Cruzado, G., Mayta-Apaza, A., Giusti, M., Jiménez-Flores, R., & García-Cano, I. (2021). Invited review: Acid whey trends and health benefits. In *Journal of Dairy Science* (Vol. 104, Issue 2, pp. 1262–1275). Elsevier Inc. https://doi.org/10.3168/jds.2020-19038

Samal, S. K., Dash, M., Vlierberghe, S. Van, Kaplan, D. L., Chiellini, E., Blitterswijk, C. van, Moroni, L., & Dubruel, P. (2012). Cationic polymers and their therapeutic

potential. *Chemical Society Reviews*, *41*(21), 7147–7194. https://doi.org/10.1039/c2cs35094g

Santos, J. C. S. D., Barbosa, O., Ortiz, C., Berenguer-Murcia, A., Rodrigues, R. C., & Fernandez-Lafuente, R. (2015). Importance of the Support Properties for Immobilization or Purification of Enzymes. *ChemCatChem*, *7*(16). https://doi.org/10.1002/cctc.201500310

Schreiber, F. (2004). Self-assembled monolayers: From “simple” model systems to biofunctionalized interfaces. *Journal of Physics Condensed Matter*, *16*(28). https://doi.org/10.1088/0953-8984/16/28/R01

Secundo, F. (2013). Conformational changes of enzymes upon immobilisation. *Chemical Society Reviews*, *42*(15), 6250–6261. https://doi.org/10.1039/c3cs35495d

Seo, M. H., Han, J., Jin, Z., Lee, D. W., Park, H. S., & Kim, H. S. (2011). Controlled and oriented immobilization of protein by site-specific incorporation of unnatural amino acid. *Analytical Chemistry*, *83*(8). https://doi.org/10.1021/ac103334b

Sheldon, R. A. (2011). Characteristic features and biotechnological applications of cross-linked enzyme aggregates (CLEAs). In *Applied Microbiology and Biotechnology* (Vol. 92, Issue 3, pp. 467–477). https://doi.org/10.1007/s00253-011-3554-2

Sheldon, R. A., & van Pelt, S. (2013). Enzyme immobilisation in biocatalysis: Why, what and how. *Chemical Society Reviews*, *42*(15). https://doi.org/10.1039/c3cs60075k

Shurson, J. (2009). *What we know about feeding liquid by-products to pigs.* https://www.thepigsite.com/articles/what-we-know-about-feeding-liquid-byproducts-to-pigs

Sirisha, V. L., Jain, A., & Jain, A. (2016). Enzyme Immobilization: An Overview on Methods, Support Material, and Applications of Immobilized Enzymes. In *Advances in Food and Nutrition Research* (Vol. 79, pp. 179–211). Academic Press Inc. https://doi.org/10.1016/bs.afnr.2016.07.004

Smith, M. T., Wu, J. C., Varner, C. T., & Bundy, B. C. (2013). Enhanced protein stability through minimally invasive, direct, covalent, and site-specific immobilization. *Biotechnology Progress*, *29*(1), 247–254. https://doi.org/10.1002/btpr.1671

Smithers, G. W. (2015). Whey-ing up the options - Yesterday, today and tomorrow. In *International Dairy Journal* (Vol. 48). https://doi.org/10.1016/j.idairyj.2015.01.011

Sobiesiak, M. (2019). Analysis of structure and properties of DVB–GMA based porous polymers. *Adsorption*, *25*(3), 257–266. https://doi.org/10.1007/s10450-018-9998-2

Talasaz, A. A. H., Nemat-Gorgani, M., Liu, Y., Ståhl, P., Dutton, R. W., Ronaghi, M., & Davis, R. W. (2006). Prediction of protein orientation upon immobilization on biological and nonbiological surfaces. *Proceedings of the National Academy of*

Sciences of the United States of America, *103*(40). https://doi.org/10.1073/pnas.0605841103

Talbert, J. N., & Goddard, J. M. (2012). Enzymes on material surfaces. In *Colloids and Surfaces B: Biointerfaces* (Vol. 93, pp. 8–19). https://doi.org/10.1016/j.colsurfb.2012.01.003

Talbert, J. N., & Goddard, J. M. (2013). Influence of nanoparticle diameter on conjugated enzyme activity. *Food and Bioproducts Processing*, *91*(4), 693–699. https://doi.org/10.1016/j.fbp.2013.08.006

Teles, F. R. R., & Fonseca, L. P. (2008). Applications of polymers for biomolecule immobilization in electrochemical biosensors. In *Materials Science and Engineering C* (Vol. 28, Issue 8, pp. 1530–1543). https://doi.org/10.1016/j.msec.2008.04.010

Tu, C., Lu, H., Zhou, T., Zhang, W., Deng, L., Cao, W., Yang, Z., Wang, Z., Wu, X., Ding, J., Xu, F., & Gao, C. (2022). Promoting the healing of infected diabetic wound by an anti-bacterial and nano-enzyme-containing hydrogel with inflammation-suppressing, ROS-scavenging, oxygen and nitric oxide-generating properties. *Biomaterials*, *286*. https://doi.org/10.1016/j.biomaterials.2022.121597

Ulman, A. (1996). *Formation and Structure of Self-Assembled Monolayers*. https://pubs.acs.org/sharingguidelines

USA EPA. (1999). *Multimedia Environmental Compliance Guide for Food Processors*.

Van De Wetering, P., Moret, E. E., Schuurmans-Nieuwenbroek, N. M. E., Van Steenbergen, M. J., & Hennink, W. E. (1999). Structure-activity relationships of water-soluble cationic methacrylate/methacrylamide polymers for nonviral gene delivery. *Bioconjugate Chemistry*, *10*(4), 589–597. https://doi.org/10.1021/bc980148w

Vukoje, I. D., Džunuzović, E. S., Vodnik, V. V., Dimitrijević, S., Ahrenkiel, S. P., & Nedeljković, J. M. (2014). Synthesis, characterization, and antimicrobial activity of poly(GMA-co-EGDMA) polymer decorated with silver nanoparticles. *Journal of Materials Science*, *49*(19), 6838–6844. https://doi.org/10.1007/s10853-014-8386-x

Walden, G., Liao, X., Riley, G., Donell, S., Raxworthy, M. J., & Saeed, A. (2019). Synthesis and Fabrication of Surface-Active Microparticles Using a Membrane Emulsion Technique and Conjugation of Model Protein via Strain-Promoted Azide-Alkyne Click Chemistry in Physiological Conditions. *Bioconjugate Chemistry*, *30*(3), 531–535. https://doi.org/10.1021/acs.bioconjchem.8b00868

Walle, T. (2009). Methylation of dietary flavones increases their metabolic stability and chemopreventive effects. In *International Journal of Molecular Sciences* (Vol. 10, Issue 11). https://doi.org/10.3390/ijms10115002

Wang, G., Wang, H., Chen, Y., Pei, X., Sun, W., Liu, L., Wang, F., Umar Yaqoob, M., Tao, W., Xiao, Z., Jin, Y., Yang, S. T., Lin, D., & Wang, M. (2021). Optimization and

comparison of the production of galactooligosaccharides using free or immobilized Aspergillus oryzae β-galactosidase, followed by purification using silica gel. *Food Chemistry*, *362*. https://doi.org/10.1016/j.foodchem.2021.130195

Wei, S., & Knotts, T. A. (2011). Effects of tethering a multistate folding protein to a surface. *Journal of Chemical Physics*, *134*(18). https://doi.org/10.1063/1.3589863

Wu, J. C. Y., Hutchings, C. H., Lindsay, M. J., Werner, C. J., & Bundy, B. C. (2015). Enhanced Enzyme Stability Through Site-Directed Covalent Immobilization. *Journal of Biotechnology*, *193*, 83–90. https://doi.org/10.1016/j.jbiotec.2014.10.039

Yang, R., Asatekin, A., & Gleason, K. K. (2012). Design of conformal, substrate-independent surface modification for controlled protein adsorption by chemical vapor deposition (CVD). In *Soft Matter* (Vol. 8, Issue 1, pp. 31–43). https://doi.org/10.1039/c1sm06334k

Yang, R., & Gleason, K. K. (2012). Ultrathin antifouling coatings with stable surface zwitterionic functionality by initiated chemical vapor deposition (iCVD). *Langmuir*, *28*(33), 12266–12274. https://doi.org/10.1021/la302059s

Yılmaz, K., Şakalak, H., Gürsoy, M., & Karaman, M. (2021). Vapor deposition of stable copolymer thin films in a batch iCVD reactor. *Journal of Applied Polymer Science*, *138*(13). https://doi.org/10.1002/app.50119

Zahirinejad, S., Hemmati, R., Homaei, A., Dinari, A., Hosseinkhani, S., Mohammadi, S., & Vianello, F. (2021). Nano-organic supports for enzyme immobilization: Scopes and perspectives. In *Colloids and Surfaces B: Biointerfaces* (Vol. 204). Elsevier B.V. https://doi.org/10.1016/j.colsurfb.2021.111774

Zakeri, B., Fierer, J. O., Celik, E., Chittock, E. C., Schwarz-Linek, U., Moy, V. T., & Howarth, M. (n.d.). *Peptide tag forming a rapid covalent bond to a protein, through engineering a bacterial adhesin*. https://doi.org/10.1073/pnas.1115485109/-/DCSupplemental

Zhuang, Z., Jewett, A. I., Soto, P., & Shea, J. E. (2009). The effect of surface tethering on the folding of the src-SH3 protein domain. *Physical Biology*, *6*(1). https://doi.org/10.1088/1478-3975/6/1/015004

Zotta, T., Solieri, L., Iacumin, L., Picozzi, C., & Gullo, M. (2020). Valorization of cheese whey using microbial fermentations. In *Applied Microbiology and Biotechnology* (Vol. 104, Issue 7). https://doi.org/10.1007/s00253-020-10408-2

Supplementary material

Table S 1.The iCVD gas flow rates for synthesizing the immobilization supports.

Polymer chemistry	Flow rates, $\boldsymbol{FR}$ (sccm)						
	Monomers				Initiator, TBPO	Carrier gas, Ar	Total
	GMA	DMAEMA	EGDMA	DVB			
pG	1.40	NA	NA	NA	0.60	1.00	3.00
pGE(25)	0.90	NA	0.10	NA	0.60	1.40	3.00
pGB(25)	1.33	NA	NA	1.10	0.60	0.00	3.27
pGD(25)	2.00	0.60	NA	NA	0.60	0.00	3.20
pGD(65)	1.00	1.00	NA	NA	0.60	0.40	3.00
pGDB	1.00	1.00	NA	0.34	0.60	0.00	2.94
pGDE	2.00	2.00	0.07	NA	0.60	0.00	4.67

Table S 2. The process parameters of the iCVD depositions for synthesizing the immobilization supports.

Polymer chemistry	P_m/P_{sat} on iCVD stage					Deposition rates (nm min^{-1})	
	GMA	DMAEMA	EGDMA	DVB	Total	DR_{stg} *	DR_{plt} *
pG	0.16	NA	NA	NA	0.16	19.23 ± 0.63	4.00 ± 0.19
pGE(25)	0.03	NA	0.10	NA	0.13	2.00 ± 0.07	0.40 ± 0.01
pGB(25)	0.05	NA	NA	1.14	1.19	3.51 ± 0.03	0.86 ± 0.02
pGD(25)	0.07	0.07	NA	NA	NA	96.51 ± 1.37	5.74 ± 0.35
pGD(65)	0.04	0.13	NA	NA	0.17	46.07 ± 0.75	0.49 ± 0.02
pGDB	0.04	0.13	0.04	NA	0.21	3.70 ± 0.17	1.20 ± 0.02
pGDE	0.05	0.17	0.05	NA	0.27	32.16 1.47	7.90 ± 0.38

*DR_{stg} denotes the deposition rates measured on a Si substrate placed on the iCVD stage; DR_{plt} denotes those measured on a Si substrate located atop the 96-well plates, which were placed on the custom-made aluminum plates on the iCVD stage.

Table S 3. Copolymer molar composition from FTIR.

Copolymer	ID	G	D	E	B
P(GMA-co-EGDMA)	pGE(25)	74	na	26	na
P(GMA-co-DVB)	pGB(25)	75	na	na	25
P(GMA-DMAEMA) (1:3.3 Pm/Psat ratio)	pGD(65)	35	65	na	na
P(GMA-DMAEMA) (1:1:1 Pm/Psat ratio)	pGD(25)	76	24	na	na
P(GMA-co-DMAEMA-co-EGDMA) (1:3.3:1 Pm/Psat ratio)	pGDE	49	37	14	na
P(GMA-co-DMAEMA-co-DVB) (1:3.3:1 Pm/Psat ratio)	pGDB	32	58	na	11

Table S 4. Random Immobilization Yield (IY)

LacZ Microenvironment	No. LacZ-WT immobilized /100nm^2	IY(%)
RI-pG	48.50 ± 4.58	8.59 ± 0.81
RI-pGE(25)	43.15 ± 3.00	7.64 ± 0.53
RI-pGB(25)	50.08 ± 4.99	8.87 ± 0.88
RI-pGD(25)	51.02 ± 1.97	9.04 ± 0.35
RI-pGD(65)	50.39 ± 6.28	8.93 ± 1.11
RI-pGDE	51.02 ± 4.85	9.04 ± 0.86
RI-pGDB	57.64 ± 4.65	10.21 ± 0.82
RI-SG	51.34 ± 5.38	9.09 ± 0.95
RI-SGD(25)	61.73 ± 5.17	10.93 ± 0.91

Table S 5. Direct Immobilization Yield (IY)

LacZ Microenvironment	No. SC immob. /100nm^2	No. LacZ-ST immob. /100nm^2	Percentage of SC occupied by ST(%)	Yield (%)
DI-pG	111.27± 2.10	9.14 ± 1.38	8.21 ± 1.24	2.48 ± 0.37
DI-pGE(25)	128.76 ± 8.25	4.20 ± 1.08	2.94 ± 0.75	1.14 ± 0.29
DI-pGB(25)	110.57 ± 16.14	3.21 ± 1.08	2.90 ± 0.97	0.87 ± 0.29
DI-pGD(25)	77.68 ± 5.28	4.20 ± 0.65	5.41 ± 0.84	1.14 ±0.18
DI-pGD(65)	65.78 ± 7.10	4.69 ± 0.49	7.13 ± 0.75	1.27 ± 0.13
DI-pGDE	58.78 ± 5.28	9.63 ± 0.43	16.39 ± 0.73	2.61 ± 0.12
DI-pGDB	114.77 ± 3.50	2.88 ± 0.84	2.51 ± 0.73	0.78 ± 0.23
DI-SG	125.96 ± 9.47	5.35 ± 0.70	4.25 ± 0.56	1.45 ± 0.19
DI-SGD(25)	126.66 ± 12.4	9.39 ± 0.89	7.41 ± 0.70	2.54 ± 0.24

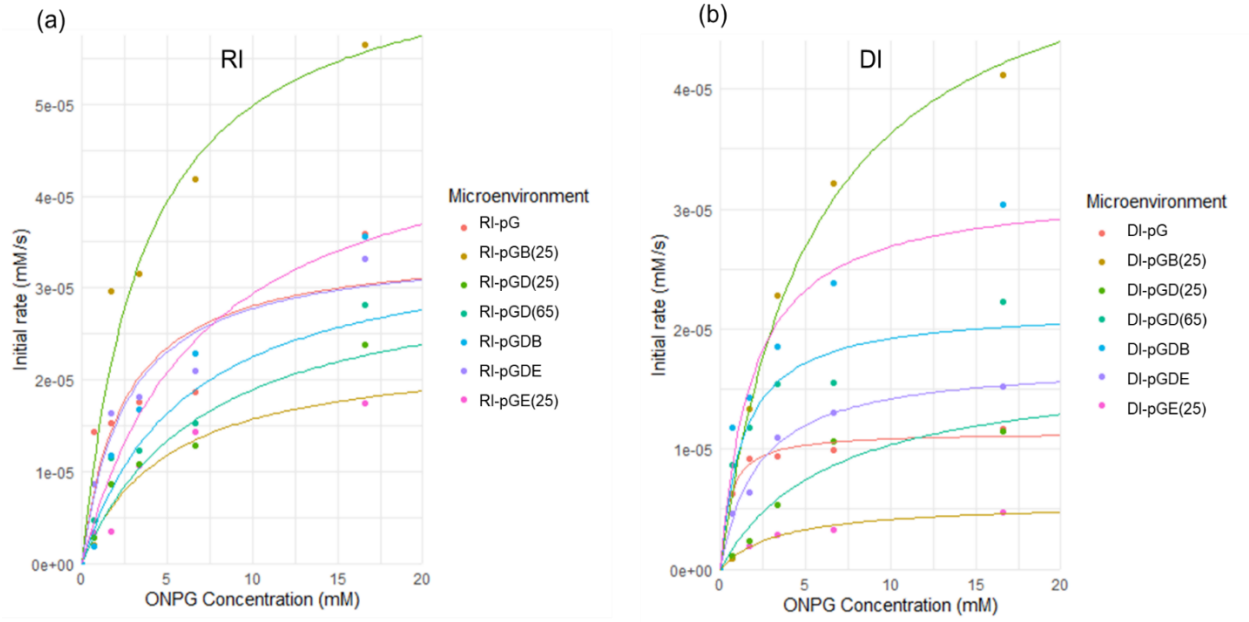

Figure S 1. Michaelis Menten plots of immobilized LacZ on different polymeric immobilization supports at pH 7 and temperature 37 ^{o}C using (a) Randomly immobilization method (b) Direct immobilization method